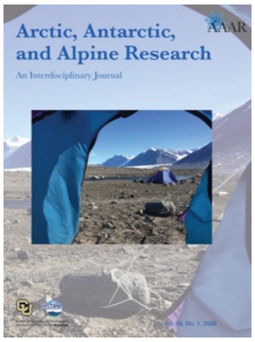

Arctic, Antarctic, and Alpine Research
An Interdisciplinary Journal

ISSN: 1523-0430 (Print) 1938-4246 (Online) Journal homepage: www.tandfonline.com/journals/uaar20

Sediment connectivity evolution in three deglaciating Alpine catchments since the Little Ice Age: A graph-based reconstruction

Toni Himmelstoss , Lena Bartram , Florian Haas , Michael Becht & Tobias Heckmann

To cite this article: Toni Himmelstoss , Lena Bartram , Florian Haas , Michael Becht & Tobias Heckmann (2026) Sediment connectivity evolution in three deglaciating Alpine catchments since the Little Ice Age: A graph-based reconstruction, Arctic, Antarctic, and Alpine Research, 58:1, 2711473, DOI: 10.1080/15230430.2026.2711473

To link to this article: https://doi.org/10.1080/15230430.2026.2711473

ARCTIC, ANTARCTIC, AND ALPINE RESEARCH
2026, VOL. 58, NO. 1, 2711473
https://doi.org/10.1080/15230430.2026.2711473

Taylor & Francis
by informa

OPEN ACCESS Check for updates

AAAR

Sediment connectivity evolution in three deglaciating Alpine catchments since the Little Ice Age: A graph-based reconstruction

Toni Himmelstoss, Lena Bartram, Florian Haas, Michael Becht, and Tobias Heckmann

Chair of Physical Geography, Catholic University of Eichstätt-Ingolstadt, Eichstätt, Germany

ABSTRACT

Climate-driven glacier retreat is reorganizing sediment cascades across Alpine catchments. However, what remains poorly quantified is how their structural connectivity—the spatial configuration of landforms and pathways along which sediment can be transferred—evolves over deglaciation timescales. We reconstruct structural connectivity evolution in three glaciated catchments of the European Alps (i.e. Grastal, Kaunertal, Martelltal) over ~150 years since the Little Ice Age, using graph-based analysis of sediment cascade networks in which landforms are nodes and sediment pathways directed edges. Graphs were derived from multitemporal geomorphological maps combining historical maps, terrestrial photographs, Structure-from-Motion multi-view stereo (SfM-MVS) photogrammetry, and Airborne Laser Scanning (ALS)–derived DEMs, extending reconstruction to the 1870s–1890s. Despite similar deglaciation forcing, the three catchments followed divergent trajectories, with sources, links, and barriers evolving along site-specific rather than common paths. Changes were non-linear and episodic: glacier recession produced threshold-like reorganizations at Kaunertal and Grastal near the turn of the millennium, once retreating glaciers crossed topologically significant boundaries. Barrier positioning, not abundance, controlled system-scale filtering: a single strategically located lake in Grastal intercepted more sediment pathways than 13 lakes in Martelltal. Event-based routing showed connectivity increased in Kaunertal but declined in the other two via different mechanisms, indicating that network restructuring can outweigh source expansion in setting potential sediment delivery.

ARTICLE HISTORY
Received 2 February 2026
Revised 19 July 2026
Accepted 26 July 2026

KEYWORDS
Sediment connectivity; graph analysis; climate change; geomorphological maps; alpine catchments

Introduction

Climate-driven glacier retreat is transforming alpine catchments into rapidly adjusting proglacial systems that affect water and sediment fluxes beyond their headwater areas (Heckmann, Morche, and Becht 2019; Carrivick and Tweed 2021; Zhang et al. 2022). Deglaciation exposes previously ice-covered terrain to subaerial processes, reorganizes sediment storage and transfer pathways, and initiates paraglacial adjustments expected to dominate sediment supply and landscape change in mid- to high-latitude mountain regions over the coming centuries (Ballantyne 2002; Knight and Harrison 2014). Whether and how rapidly these adjustments propagate downstream depends not only on sediment availability at exposed sources but also on the structural configuration of the cascade through which sediment must travel. Altered sediment export affects downstream river morphodynamics, reservoir sedimentation, flood mitigation infrastructure, water quality, and ecological systems (Carrivick and Tweed 2021; Zhang et al. 2022).

The propagation of such geomorphic changes through mountain catchments is moderated by sediment connectivity, defined as the degree to which a system facilitates sediment transfer through itself (Heckmann et al. 2018). Proglacial margins contain abundant sediment sources: oversteepened slopes, moraines, debris cones, fluvial deposits, and weathered bedrock (Ballantyne 2002; Carrivick and Heckmann 2017; Betz-Nutz et al. 2023). Storage landforms can themselves become active sources through gully erosion, fluvial undercutting, or debris flows (Haas et al. 2012; Mancini and Lane 2020). Whether mobilized sediments reach downstream areas, however, depends on the spatial configuration of landforms acting as buffers, barriers, or links within sediment cascades (Fryirs et al. 2007a; Cavalli, Heckmann, and Marchi 2019).

CONTACT Toni Himmelstoss Toni.Himmelstoss@posteo.de Chair of Physical Geography, Catholic University of Eichstätt-Ingolstadt, Eichstätt, Germany
Supplemental data for this article can be accessed online at https://doi.org/10.1080/15230430.2026.2711473

Sediment connectivity evolves over time: Structural changes such as drainage reorganization, lake formation and infilling, and the de- or recoupling of system components occur frequently in proglacial environments (Bennett et al. 2010; Bogen, Xu, and Kennie 2015; Shugar et al. 2017). Lane et al. (2017) suggest that while initial glacier recession may enhance sediment export through increased source-channel coupling, subsequent sediment reworking by fluvial processes can reduce downstream connectivity and shift sediment delivery toward greater dependence on extreme transport events. Understanding these dynamics benefits from distinguishing structural and functional connectivity (Turnbull, Wainwright, and Brazier 2008; Wainwright et al. 2011): Structural connectivity describes the spatial configuration of potential sediment pathways—the physical arrangement of sources, transfer zones, and sinks. Functional connectivity refers to actual sediment transfer under specific forcing conditions along these pathways. Both are challenging to quantify over timescales relevant to global warming. Functional connectivity assessment is hampered by the scarcity of long-term in situ sediment flux measurements (Orwin et al. 2010), while approaches based on elevation differencing face substantial uncertainties from unknown subglacial contributions, infrequent surveys, and confounding signals such as dead ice melt (Hilger and Beylich 2019; Piermattei et al. 2023; Savi et al. 2023; Bayens et al. 2025). Structural connectivity assessment with widely used approaches such as the Index of Connectivity (Cavalli et al. 2013) is likewise constrained by the need for consistent, high-quality elevation data over decadal timescales. While digital elevation models (DEMs) derived from historical aerial imagery have enabled studies extending to the 1950s, data quality varies considerably (Micheletti, Lane, and Chandler 2015; Stark et al. 2022; Marty et al. 2025).

Graph theory offers a promising framework for addressing some of these limitations. Representing the sediment cascade as a graph in which landforms are nodes and possible sediment transfer pathways are directed edges renders system topology explicit and amenable to standard methods of network analysis (Heckmann, Schwanghart, and Phillips 2015; Hooke and Souza 2021), providing a framework for tracking the propagation of perturbations through sediment systems (Cossart and Fressard 2017; Fressard and Cossart 2019). Graphs can be constructed from diverse input data (Heckmann and Schwanghart 2013; Buter et al. 2022), enable analysis of both structural (Fressard and Cossart 2019) and functional connectivity (Hiatt, Addink, and Kleinhans 2022; Himmelstoss et al. 2024), and can be applied across spatiotemporal scales (Phillips, Schwanghart, and Heckmann 2015; Lehotský et al. 2018). Heckmann and Schwanghart (2013) demonstrated an early application where raster cells served as nodes and modeled sediment trajectories as edges, enabling explicit treatment of sources, sinks, and cascading pathways. More recently, sediment cascades have been mapped and represented as graphs using geomorphological maps (Buter et al. 2020, 2022). However, geomorphological maps (GMs) of proglacial areas remain rare, typically cover single sites at single timeframes, and require substantial resources to produce (Carrivick and Heckmann 2017), which has limited the multi-catchment comparisons across geological and climatic settings needed to test conceptual models of proglacial landscape development quantitatively.

Few studies have investigated the evolution of individual deglaciating systems over decadal timescales (e.g., Bennett et al. 2010; Staines et al. 2015) or compared the structure of multiple geosystems characterized by recent deglaciation (e.g., Geilhausen, Otto, and Schrott 2012; Kirkbride and Deline 2018). While these studies used planform or geomorphometric analysis to describe landscape composition and evolution, they did not employ metrics that capture system topology and enable comparison across sites and time periods. Lane et al. (2017) called for combining graph theory methods with historical data on glacier extent to quantify how sediment flux had changed through time. Carrivick and Heckmann (2017) noted the potential of historical aerial photographs and maps for reconstructing proglacial system development, arguing that such studies could address questions of path dependence, topographic inheritance, and changing connectivity. A systematic, cross-site, and multi-temporal quantification of structural connectivity evolution since the Little Ice Age is, to our knowledge, still lacking. Such a reconstruction is complementary to the substantial body of work on changing source activity and sediment yield in deglaciating systems (Betz-Nutz et al. 2023; Piermattei et al. 2023; Rom et al. 2023a; Altmann et al. 2024): catchment-scale yield reflects both supply and the transmissivity of the intervening cascade (Carrivick and Tweed 2021; Zhang et al. 2022), and isolating the structural component clarifies how much of the observed variability in proglacial sediment flux can be attributed to network reorganization rather than to changing source activity.

In this study, we investigate structural changes in glaciated geosystems across three catchments in the European Alps using sediment cascade graphs derived from multitemporal geomorphological maps spanning approximately 150 years since the Little Ice Age maximum. Building on previous approaches (Messenzehl, Hoffmann, and Dikau 2014; Buter et al. 2022), we use landforms as fundamental spatial units (Poeppl and Parsons 2018). Whereas earlier studies mapped sediment pathways manually (Buter et al. 2022; Bollati et al. 2024), we developed a semi-automatic approach based on the typical functional roles that landforms assume in high alpine glaciated systems (Cavalli, Heckmann, and Marchi 2019) to enable scalability and enhance reproducibility. We focus on coarse sediment connectivity between landforms acting as sources, links, and barriers. To capture the changing structure of these deglaciating systems over time, we select and develop graph metrics that are robust against differences in data quality and network size, enabling comparison across catchments and time periods. Additionally, we implement an event-based routing approach to model network response to activation of major sediment sources during a high-magnitude event, following the modeling of hydro-meteorological scenarios in Buter et al. (2022). Together, these analyses probe the structural side of paraglacial adjustment and the variation in its trajectory between catchments under broadly similar climatic forcing. Specifically, we address the following questions:

(1) How does the structural connectivity of high alpine geosystems evolve during deglaciation? Do changes follow gradual trajectories or exhibit inflection points linked to specific landform changes?
(2) What role do barrier landforms—lakes, alluvial fans, and braidplains—play in controlling connectivity, and how does their topological importance change as proglacial areas expand?
(3) How do structural changes translate to potential sediment delivery under high-magnitude forcing?
(4) Do the three catchments exhibit convergent evolutionary patterns, or do site-specific factors drive divergent trajectories?

Study sites and methods

Study sites

We investigate and compare the structural development of three glaciated catchments in the Central European Alps: The Grastal valley (GT), a side valley of the Horlachtal valley, the Gepatschferner proglacial system in the upper Kaunertal (KT), and the Langen-, Zufall-, and Fürkeleferner proglacial system in the upper Martelltal (MT). The Kaunertal and Grastal valleys are situated in Tyrol, Austria, north of the main Alpine ridge, while the Martelltal lies in South Tyrol, Italy (Figure 1). Geologically, the Horlachtal and Kaunertal belong to the polymetamorphic Ötztal-Stubai Complex, dominated by paragneisses and orthogneisses (Becht 1995; Vehling 2016), whereas the Martelltal is part of the Ortler-Campo Crystalline Complex, characterized by quartz phyllites (Martin et al., 2009).

The study sites were selected because all three remain glaciated at present, are relatively undisturbed by direct anthropogenic modification, and maintained coarse sediment connectivity to their respective catchment outlets throughout the investigation period. Important study site characteristics are presented in Table 1. The main rivers in the upper Kaunertal (Fagge) and upper Martelltal (Plima) drain into reservoirs, while the Grastalbach drains into the Ötztaler Ache, a tributary of the Inn. The KT and MT study sites are delimited by the maximum Little Ice Age (LIA) glacier extent and thus comprise both glaciers and proglacial areas (Figure 1). The GT study site extends beyond the proglacial area because glacier retreat triggered major drainage network reorganization through landforms outside the LIA boundary—a configuration absent in KT and MT. Additionally, debris flow activity originating from hillslopes beyond the proglacial area plays a substantial role in the valley's sediment budget (Rom et al. 2023a; Himmelstoss et al. 2024) and responds to glacier dynamics (Rom et al. 2023b).

While the Martelltal has a leveled topography with extensive ground moraine areas (3.76 km^2 or 41 percent of the proglacial area in 2019), the Gepatschferner proglacial area in Kaunertal is dominated by large lateral moraines (1.68 km^2 in 2017) and roche moutonnées (0.46 km^2) in the valley bottom of the Gepatschferner tongue (GZ). Larger ground moraine areas can be found in the western part of the KT study site though (the so-called Nördergries, NG) covering 1.18 km^2. In the lower part of the Grastal valley, talus slopes (1.75 km^2) below rockwalls shape the landscape, often reaching close to the Grastalbach stream. The proglacial area consists largely of glacially eroded bedrock and rock face (0.31 km^2 or 74 percent in 2017), two lateral moraines and a breached terminal moraine. Dominant sediment sources reflect these morphological differences: in the upper Kaunertal, the Gepatschferner glacier and fluvial erosion are the primary contributors (Hilger et al., 2019), and in Grastal debris flows and fluvial erosion play a prominent role (Himmelstoss et al. 2024). No comparable sediment budget study exists for Martelltal; however, glaciers, moraines, and fluvial channels were identified as principal sources in the adjacent Suldental (Savi et al. 2024).

Hydrological regimes differ among sites in ways relevant to their paraglacial stage. Kaunertal shows increasing annual discharge with no indication that peak water

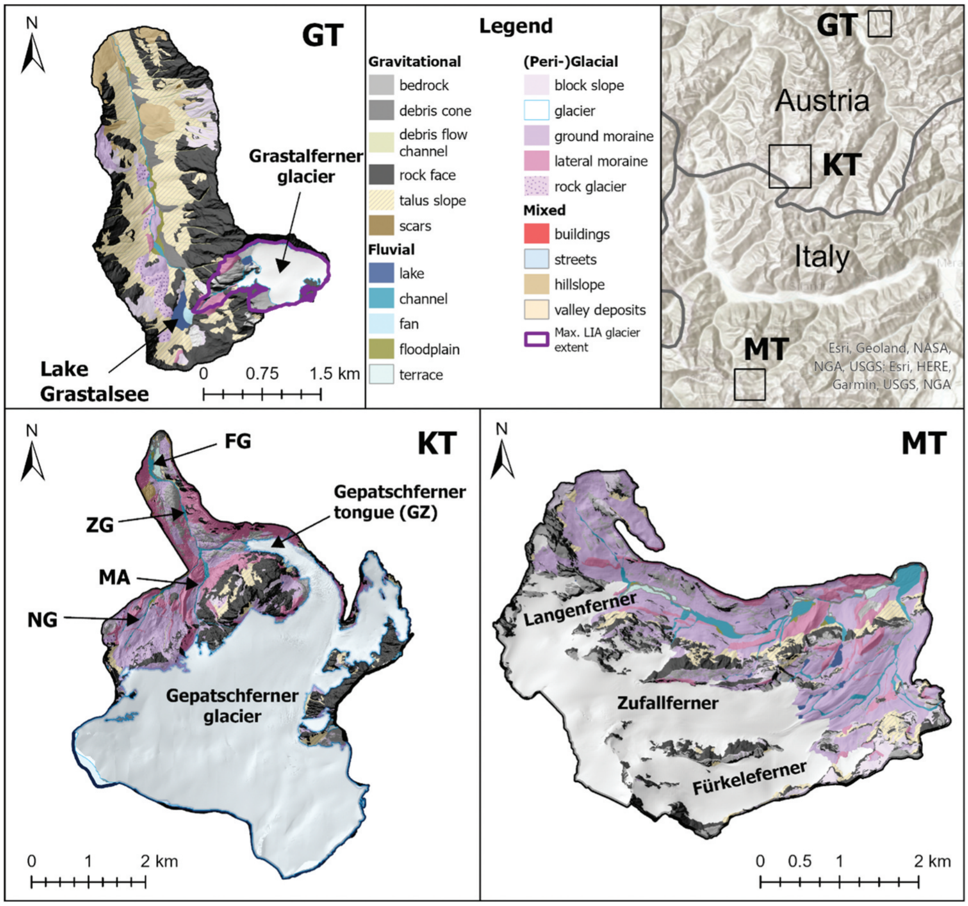

Figure 1. Location and overview of the three study sites. Recent geomorphological maps as overlay, hillshade in the background. Glaciers and other important features are marked or abbreviated. FG = "Fernergries," ZG = "Zwischengries," MA = "Münchner Abfahrt," NG = "Nördergries."

Table 1. Morphometry, glaciation and climate characteristics of the three study sites.

	Grastal	Kaunertal	Martelltal
Location	11.00°E 47.11°N	10.75°E 46.85°N	10.64°E 46.46°N
Study site area	7.2 km^2	23.5 km^2	15.2 km^2
Elevation range	1,933–3,339 m.a.e.	1,960–3,547 m.a.e.	2,372–3,809 m.a.e.
Mean slope	0.84 m/m	0.40 m/m	0.50 m/m
with/without glacier	0.88 m/m	0.70 m/m	0.57 m/m
Glaciation (max. LIA)	0.97 km^2	22.2 km^2	14.1 km^2
Glaciation (recent)	0.49 km^2 (2022)	14.9 km^2 (2021)	8.8 km^2 (2021)
Glacier loss (area)	0.48 km^2/49%	7.3 km^2/33%	5.3 km^2/38%
Mean Temp.	3.1°C	2.7°C	2.9°C
	(1990–2019, Horlachalm, 1,910 m)	(2010–2020, Gepatschalm, 1,900 m)	(1981–2010, Zufrittsee 1,851 m)
Mean annual precipitation	817 mm	1,089 mm	750 mm
	(1990–2019, Horlachalm)	(2010–2023, Gepatschalm)	(1980–2010, Zufrittsee)

has been reached, based on discharge records from Tiroler Wasserkraft AG (TIWAG; Gepatschalm gauge, 1971–2024). In the Horlachtal, declining summer discharge and reduced diurnal variability suggest a diminishing glacial component (discharge records at TIWAG Fassung Horlach, 1985–2022), matching the late-stage entropy signature Lane and Nienow (2019) describe for glaciated basins in which ice cover has dropped below the threshold for a dominant ice-melt subsidy. Evidence for Martelltal remains inconclusive with model data showing decreasing rainfall and snowmelt contributions but increasing glacier melt (Fan et al. 2025), though neighboring catchments may have passed peak water (Savi, Dinale, and Comiti 2021, 2024). These hydrological differences have implications for sediment transport regimes: in glacier-dominated catchments such as Kaunertal and Martelltal, bedload transport is controlled primarily by glacier melt dynamics rather than precipitation, with bedload concentrations during glacier melt exceeding those during snowmelt by orders of magnitude, as demonstrated for a neighboring catchment (Comiti et al. 2019).

Geomorphological mapping and backdating

Geomorphological mapping draws on four data-source classes, spanning approximately 150 years: Airborne Laser Scanning (ALS)–derived orthophotos and DEMs for the most recent time steps, Structure-from-Motion multi-view stereo (SfM-MVS) products from historical aerial imagery (1945–1997), historical topographic maps (1870s–1930s), and historical terrestrial photographs. A complete inventory is given in Figure 2 and Appendix B and each source class is described below. Existing geomorphological maps from the three study sites were harmonized into 20 classes representing gravitational, fluvial, glacial, periglacial, and anthropogenic landforms (see Appendix A for full catalog). The maps have a target scale of 1:5,000 and consist of polygons seamlessly covering the entire study sites. Mapping was supported by hillshades, slope maps, orthomosaics, and DEMs of Differences (DoDs).

For each study site, the most recent geomorphological map serves as the base map: it is derived from the highest-quality data (ALS-DEMs and orthophotos) and constitutes the starting point from which all earlier maps were produced by backdating. The Kaunertal base map was created during a previous project (Hilger 2017; Hilger and Beylich 2019) and updated to 2017 using ALS data and orthophotos. The base maps of the Grastal Valley (2017) and Martelltal Valley (2019) were created by the authors. For maps depicting conditions after 2000, orthophotos and DEM derivatives from ALS surveys were used. Sources were the State of Tyrol (data.tirol.gv.at) and the Autonomous Province of Bozen (natur-raum.provinz.bz.it), except for the KT 2017 and MT 2019 ALS data, which were acquired by the authors. Starting from the base map, landform boundaries were then progressively adjusted to represent earlier stages, in chronological steps, based on historical data sources.

The mapped channel network was longitudinally subdivided into reaches, delimited by significant changes in slope gradient or confinement, as well as upstream of confluences. This delimitation was chosen because such reaches can be readily classified according to their function within the sediment cascade—as sources, links, or sinks—although this function may shift over time (Piermattei et al. 2023). Their spatial extent also makes them suitable as fundamental units for graph analysis (Himmelstoss et al. 2024). Laterally, the reaches comprise the entire active channel including gravel bars and small islands.

Aerial imagery and SfM-products (1945–1997)

Historical aerial images were processed using SfM-MVS -photogrammetry to derive orthomosaics and DEMs for time steps between 1945 and 1997. The processing workflow is described in detail by Stark et al. (2022), with dataset quality assessed for Kaunertal by Piermattei et al. (2023). The Horlachtal SfM datasets were processed by project members using the same SfM-MVS workflow and are of comparable quality. The orthoimages were previously used for debris flow mapping (Rom et al. 2023a). For both sites, the original images were sourced from the Province of Tyrol or the Austrian “Bundesamt für Eich- und Vermessungswesen” (BEV).

For Martelltal, the historical aerial images 1945 and 1969 were sourced from the Italian Military Geographic Institute (IGMI) and processed using the same workflow. However, the lower quality of the original images results in higher positional uncertainty for smaller

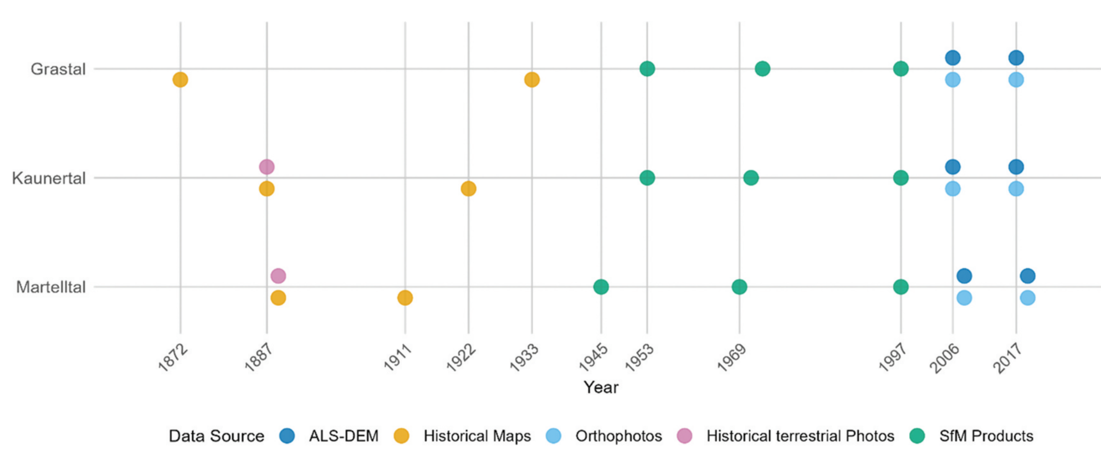

Figure 2. Timeline with the central data sources used for geomorphological mapping and backdating. SfM Products include both the DEM and orthomosaic.

landforms. Orthoimages from 1997 onwards were derived from the Autonomous Province of Bozen/Bolzano. Quality metrics (ground sampling distance, GSD; and tie-point root-mean-square error, RMSE) for all self-processed SfM datasets are listed in Appendix C.

Historical maps (1872–1933)

Since overlapping aerial photographs of our study sites date back only to the 1940s, historical maps were used to extend the geomorphological record further back in time. Especially the maps by S. Finsterwalder (KT 1887, KT 1922, MT 1889) show considerable detail in their depiction of glacier extent and channel networks. Appendix D lists the historical maps used for each study site. Where several historical maps were combined for a single geomorphological map, the assigned year corresponds to the source with the highest level of detail. Where the date of the underlying field survey differs from the publication date, the survey date was used (e.g., GT 1933, based on the "Map of the Stubai Alps" published in 1939).

Historical terrestrial photographs

Historical terrestrial photographs were used primarily to verify information from historical maps and to obtain additional detail on channel morphology—for instance, to supplement spatially limited maps with views of glacier tongues or channel reaches outside the mapped extent (Figure 3). Image orientation and monoplotting were performed using the open-source tool MoniQue (Mikolka-Flöry, Ressl, and Pfeifer 2025; github.com/smfloery/moniQue).

Sediment source mapping

The primary data source for sediment source mapping were catchment-wide DoDs from the subsequent period of the GM, e.g., the Grastal DoD 1973–1953 for GT 1953. As input we used both SfM-derived and ALS-

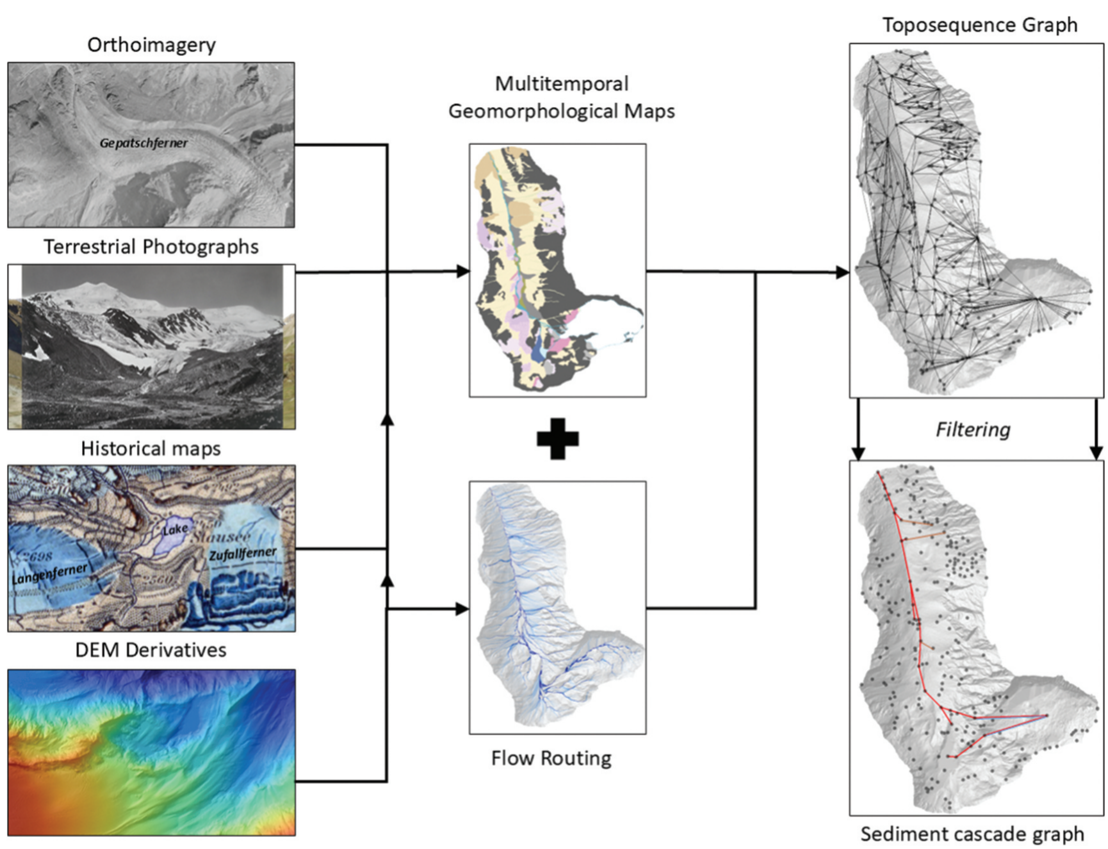

Figure 3. Workflow for constructing sediment cascade graphs. Input data (left): historical aerial imagery (KT, 1953), terrestrial photographs (MT, ca. 1890), historical maps (MT, 1911), DEM Derivatives (MT 2019) used for geomorphological mapping and backdating. Combined with a hydrologically corrected DEM, the "Flow between fields" SAGA tool produces a toposequence graph in which landforms are nodes and edges record flow routing between adjacent polygons (top right). Rule-based filtering then retains sediment sources coupled to the linking landforms, river reaches, and barrier landforms (lakes, braidplains, alluvial fans), removing uncoupled landforms and redundant edges to yield the sediment cascade graph (bottom right). Graph construction shown for GT 1933.

derived DEMs as listed in Figure 2. For the most recent GMs, we used ALS DEMs from 2023 based on our own aerial surveys, e.g., MT 2023–2019 for the MT 2019 map. All pairs of DEMs were coregistered with demcoreg using the Nuth and Kääb algorithm (Nuth and Kääb 2011; Shean et al. 2016). For all study sites, we began the source mapping with the ALS-born DoDs, as those are most reliable regarding data quality.

Based on this, multi-stage sediment source mapping was carried out:

(1) Glacier portals draining into a river channel were classified as sediment sources by rule given their large contribution in sediment budget studies (Hilger and Beylich 2019).
(2) Potential hillslope sediment sources in proximity to the channel network were analyzed with DoDs. This primarily targeted continuously active proglacial lateral moraines, which can achieve mean annual sediment output of several hundred cubic meters per year (Altmann et al. 2024). We preselected landforms with a net erosion exceeding 1,000 m^3 over the respective DoD period as a practical threshold to focus on geomorphologically significant sources and then determined based on the spatial patterns in the DoD, the landform characteristics, the location and surroundings whether it was actually a sediment-supplying unit or whether the DoD was indicating another signal (e.g., dead ice melt, snow melt).
(3) The channel network was analyzed reach-by-reach whether substantial lateral erosion or incision (>1,000 m^3) occurred during the time period. As geomorphological maps are a snapshot from the beginning of the DoD-time span and the channels shift or expand over time, we could not rely solely on the net balance of the individual reaches but had to include the adjacent eroding landforms (often ground moraine or lateral moraines) as well.
(4) We examined the DoDs for landforms indicative of low-frequency, high-magnitude activity (e.g., rockfall and landslide deposits, debris-flow channels). As each DoD integrates all surface change between two survey epochs, a single mapped deposit may aggregate the products of several individual events. We distinguished between deposits of processes likely to occur only once during the entire period (e.g., large rockfalls or landslides) and landforms shaped by recurring processes such as debris flows. The former were only mapped as sediment sources for the corresponding time step, while debris flow channels with repeat sediment delivery to the channel network were marked as sources for all time steps.

With variable data availability, the mapping of sediment sources had to be adjusted for older GMs.

Step 1 could be performed for all data sources, as glaciers and channels were also included in the historical maps. Step 2 relies on DoDs and could not be repeated in the same manner for the two oldest GMs. Betz-Nutz et al. (2023) investigated lateral moraine activity in ten proglacial areas since the 1950s, finding slight decreases in erosion rates over time in most cases. Altmann et al. (2024) similarly found decreasing erosion rate trends in 10 of 12 lateral moraine sections. Consequently, we assume that moraines continuously mapped as sediment sources were also active during the two prior time periods, if a) they were not covered by glacier and b) the nearby channels were in a similar location. Step 3 also could not be repeated with DoDs for the two earliest GMs. In the Kaunertal and Martelltal valleys, glaciers covered most of the area, and the mapping of the remaining channels indicated a braiding morphology, so no reach was classified as sediment source. The river reach with the highest erosion in Grastal became active much later (1997 onwards), and the channel was not at the same location according to the oldest historical maps, so we did not map channel sources for the first two time steps either.

Regarding step 4, Rom et al. (2023a, 2023b) found no long-term trend in the frequency of extreme debris flow events in the Horlachtal valley despite high short-term variability. These findings support the assumption these sediment sources identified in recent time periods can be extended to earlier periods lacking DoD coverage, provided their coupling to the active channel remained unchanged. There is little to no data available on other low-frequency high-magnitude events for the two earliest time periods. Given that landforms that were later subject to such events (like landslides and large rockfalls) were glacier-covered at this time (or glacial debuttressing was at a very early stage), the occurrence of such events is considered unlikely.

Link, barrier and sink mapping

Landforms that are neither classified as sediment sources nor part of the active fluvial system are treated as disconnected from the sediment cascade by default. This approach is supported by findings that effective sediment-contributing areas in Alpine catchments are often small, with large parts (or most landforms) remaining disconnected from the channel network

(Fryirs et al. 2007b; Heckmann and Schwanghart 2013; Altmann et al. 2021; Buter et al. 2022; Turley and Hassan 2023), including the Kaunertal (Hilger and Beylich 2019) and Grastal (Himmelstoss et al. 2024) valleys. Within the fluvial system, river reaches are treated as links that transport sediment downstream. Three landform classes act as barriers to coarse sediment transfer. Lakes are treated as complete bedload sinks given the size and inflow characteristics of the proglacial lakes in the study catchments (Geilhausen et al. 2013; Bogen, Xu, and Kennie 2015). Braidplains transmit suspended load but filter and delay bedload (Mancini et al. 2023). Multi-decadal DoD analyses across the three study sites show that proximal braidplains function as net sinks while distal braidplains approach transport equilibrium (Rom et al. in review). Alluvial fans reduce downstream sediment flux through diffusive deposition (Mancini and Lane 2020). All three barrier classes are assigned filter coefficients for sediment routing. The coefficient values and their empirical basis are given in Section "Event-based sediment routing", their limitations are further discussed in Section "Methodological considerations".

Graph creation

The sediment cascade is represented as a directed graph in which nodes correspond to individual geomorphological landforms and edges represent potential sediment transfer pathways between them. This graph encodes which landforms can deliver material to which downstream landforms, based on topographic flow routing, without quantifying actual sediment fluxes (Figure 3). To derive this graph, we employed the "Flow between fields" tool in SAGA GIS (version 6.3.0), which implements a multiple flow direction (MFD) algorithm. This tool routes flow from DEMs through rasterized landform polygons of the geomorphological map, producing an edge list that records flow accumulation values between adjacent landform units.

The required inputs comprise derivatives of the geomorphological maps in which each landform polygon is assigned a unique identifier and hydrologically corrected DEMs. Where no elevation model from the same year as a geomorphological map was available, the temporally nearest DEM was used. Using the R package igraph (version 2.1.4; Csardi and Nepusz 2006), graphs were created from the resulting edge lists, and basic vertex attributes—centroid coordinates, landform class, and functional role (e.g., braidplain, sediment source)—were assigned.

The first result is a directed toposequence graph in which every landform is represented by a node and edges are drawn where flow routing connects two adjacent landforms. While flow accumulation values could theoretically serve as edge weights, we found this variable to be of limited utility for glaciated systems. Surface runoff is only partially determined by the contributing catchment area of each raster cell, and the capacity to transfer sediment from one node to another depends on numerous factors that cannot be readily quantified at this level of abstraction. Consequently, flow accumulation is used only for the removal of mutual edges (see below).

To derive the sediment cascade graph from the toposequence graph, we applied several filtering steps with reference to the previous source, sink and link classification: The sediment cascade graphs retains only landforms that are either a) mapped as sediment sources and coupled to the fluvial system, b) standard river reaches as main transport pathways, or c) barrier landforms classified as lakes, alluvial fans or braidplains. Graph edges from and into all other landforms are by default removed, as these either represent primary sediment buffer zones that decouple lateral connectivity or their dominant sediment transfer mechanism is negligible in the overall sediment budget (e.g. small rockfall, avalanches, creep). Where bidirectional edges exist between nodes, only the edge with greater flow accumulation is retained, to prevent incorrectly directed edges due to mapping inaccuracies. Redundant edges from non-glacier sediment sources are eliminated, such that each mapped source couples only to the landform with which it has the strongest connection (e.g. a lateral moraine to a river section directly adjacent). This prevents hillslope sources being counted multiple times in the subsequent routing analysis. If a source landform was identified as supplying sediment to several other landforms, the corresponding source landform polygon was divided. Glaciers are allowed to connect to multiple downstream nodes if they are part of the fluvial system, as they can have several tongues and portals individually contributing sediments of significant magnitude.

Critical to the analysis is the creation of two graph versions that serve distinct analytical purposes. The *routing graph* has all outgoing edges from lake nodes removed, reflecting their function as complete sediment sinks for coarse material regardless of sediment origin and enabling sediment routing calculations. The *cascade topology graph* preserves lake connectivity, allowing network topology metrics to account for the structural position of lakes within the cascade network. Unless otherwise noted, pathway metrics were calculated on the cascade topology graph, while sediment routing employed the routing graph.

Graph analysis

Graph analysis was also conducted with igraph in R. We organized the analysis into three thematic blocks addressing distinct research questions: (1) characterizing structural network evolution, (2) quantifying the positioning and importance of barrier landforms, and (3) an event-based routing model to assess the filtering of sediment delivery by network structure during high-magnitude events.

Structural network evolution

To characterize how sediment cascade structure changes through deglaciation, we selected metrics that are either inherently size-independent or can be normalized to enable comparison across networks of varying extent.

Network size itself is tracked through node count (n) and edge count (m). While these absolute values reflect the expanding proglacial area, their ratio (m/n) provides a size-independent indicator of network branching complexity.

Sediment source composition was disaggregated by type: glacier portals, hillslope sources (debris flows, lateral moraines, landslides etc.), and channel sources (reaches with incision or lateral erosion). Sources were identified based on the vertex attribute assigned during graph creation from geomorphological mapping and classified according to the landform process domain.

Pathway analysis quantifies the number of distinct routes connecting sediment sources to the catchment outlet. Using igraph's all_simple_paths() function, we enumerated all acyclic paths from each sediment source to the designated outlet vertex. For each pathway, we recorded: (i) the number of edges traversed (pathway length), which indicates the number of landform transitions – and thus potential filtering or buffering steps – between source and outlet, and (ii) whether the path actually traverses a lake or braidplain node. Note that the pathway length does not represent the Euclidean distance in physical space, but the number of edges (landform transitions) in the graph.

Barrier landform emergence and positioning

In order to track the formation of proglacial lakes and braidplains during the study period, they were counted at each time step. Only those lakes were counted that could potentially interrupt the sediment cascade, i.e., they must be connected to a link or a source landform.

The **lake-mediated pathway ratio** (LPR) expresses the proportion of source-to-outlet pathways that traverse at least one lake:

$$LPR = \frac{P_{lake}}{P_{total}}$$

where P_{lake} is the number of pathways containing a lake node and P_{total} is the total number of pathways. An analogous ratio was calculated for braidplains, abbreviated BPR for braidplain-pathway ratio. These ratios provide size-independent measures of barrier positioning within the network, distinguishing between systems where barriers occupy peripheral versus central positions.

Event-based sediment routing

To evaluate how network structure controls potential sediment delivery, we implemented a simplified routing model simulating coarse sediment transport during a hypothetical extreme precipitation event that activates all mapped sources susceptible to hydrometeorological forcing simultaneously. This approach follows the matrix formulation of Schwanghart and Kuhn (2010), adapted for sediment cascade networks with filtering landforms.

Each sediment source emits one unit along each outgoing edge. For glacier nodes, units are distributed across all outlet edges; for other sources, routing follows the single edge with highest flow accumulation weight. Sediment units propagate along the directed graph until reaching either the outlet or a sediment sink.

For each routing event, we calculate a routed sediment unit vector s with n elements (one per network node):

$$s = \left(I - M^T\right)^{-1} w_0$$

where I is the identity matrix, M is the weighted adjacency matrix incorporating filtering coefficients, and w_0 is the source vector (1 for source nodes, 0 otherwise). This formulation propagates source inputs through the network, applying filter coefficients at each node and summing all contributions to yield the total number of sediment units passing through each node.

Lakes are treated as complete sinks (filter coefficient = 0), retaining all incoming bedload sediment. Braidplains and alluvial fans act as partial filters with coefficients set to 0.50 and 0.45, respectively, based on the sediment delivery ratios observed during a 2022 event in the Grastal valley (Himmelstoss et al. 2024) and consistent with bedload retention values simulated by Mancini et al. (2025; reference Scenario 1) for Alpine proglacial braidplains. Given limited empirical data on bedload retention across landform types, these coefficients are treated as estimates, and we cannot quantify their temporal and spatial variability.

The matrix-based routing inherently produces cascading filtering effects: sediment passing through successive braidplains is filtered at each step, so that distal braidplains receive and retain less sediment in absolute terms than proximal ones—consistent with the spatial patterns observed in DoD-based studies of proglacial streams (see section "Barrier landform control").

The primary output metric is the **Event Delivery Ratio (EDR)**:

$$EDR = \frac{s_{outlet}}{s_{sent}}$$

where s_{outlet} is the total sediment delivery to the catchment outlet and s_{sent} is the total units dispatched from all sources. By assigning equal contributions to all sources, EDR isolates the filtering effect of network structure and barrier positioning from spatial and temporal variability in sediment availability. Additionally, we can calculate retention rates for each barrier class as the proportion of total units intercepted by lakes, alluvial fans, and braidplains, respectively: The sediment trapped in sinks is Σs_j for all sink nodes j.

Results

Structural network evolution

Number of nodes and edges

Glacier retreat and the exposure of underlying areas can drive expansion of the cascade topology graphs, but the three systems respond differently (node count n in Figure 4). All three start with relatively low counts—9 for MT, 18 for KT, and 22 for GT—and then diverge: The node count in Grastal remains nearly constant over time, which can be explained with the much smaller size of the Grastalferner glacier and the exposed proglacial areas in relation to the whole study area. Hence, if we should detect changes in pathway-related metrics, these can be attributed less to the expansion of the proglacial area visible in the lower panel of Figure 4 and more to a restructuring of the sediment cascade.

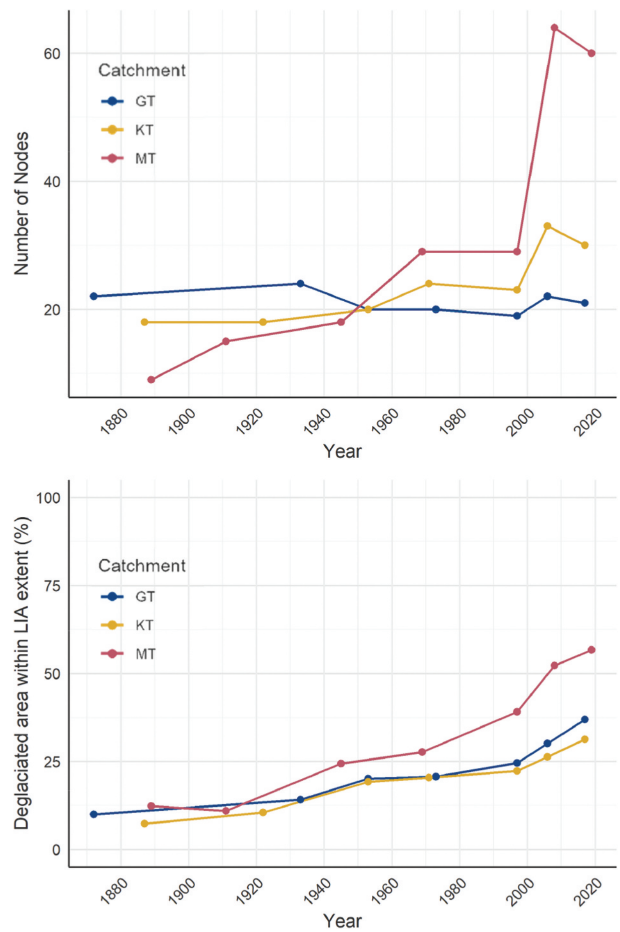

Figure 4. Upper panel: number of nodes in the sediment cascade graph at each time step for Grastal (GT), Kaunertal (KT), and Martelltal (MT). Lower panel: percentage of the maximum Little Ice Age (LIA) glacier extent that is ice-free at each time step (proglacial area).

The size of the KT cascade graph does not increase substantially over the first three time steps 1887 to 1953, as two opposing processes balance out: the melting Gepatschferner tongue exposes a confined area where the channel system lengthens without branching, while the drainage network in the Nördergries area (NG) simultaneously becomes less branched. The largest increase in network size in KT happened between 1997 and 2006, where the Gepatschferner tongue retreated behind the valley confluence and had three portals.

The MT cascade exhibited a steady increase in the first four time steps and stagnation between 1969 and 1997. We observe an inflection point with the node count increasing from 29 to 64 between the 5th and 6th time step (1997 to 2008), even though the time span is relatively short and the additional deglaciated fraction is modest compared to the magnitude of network change. The largest contribution to this was a size increase of the channel network (from 28 to 51 reaches) and the formation of a large number of additional proglacial lakes (see section "Lake emergence and pathway interception"). A slight drop of node count can be observed in the last time step across all three study sites.

The number of edges m generally develops very similarly to the number of nodes: The edge/node ratio (m/n) ranges between 1 and 1.13 for GT, between 0.98 and 1.19 for KT; both without clear temporal trends. Only MT shows an increasing trend, starting with 0.78 in 1889 and ending with 1.10 in 2019. Values below 1 indicate predominantly tree-like network structures; MT's approach to and exceedance of 1.0 reflects increasing network complexity through lateral branching in addition to longitudinal extension.

Number and composition of sediment sources

The sediment source composition plot (Figure 5) shows both different compositions and different evolution paths for the three study sites. In Grastal valley, hillslope

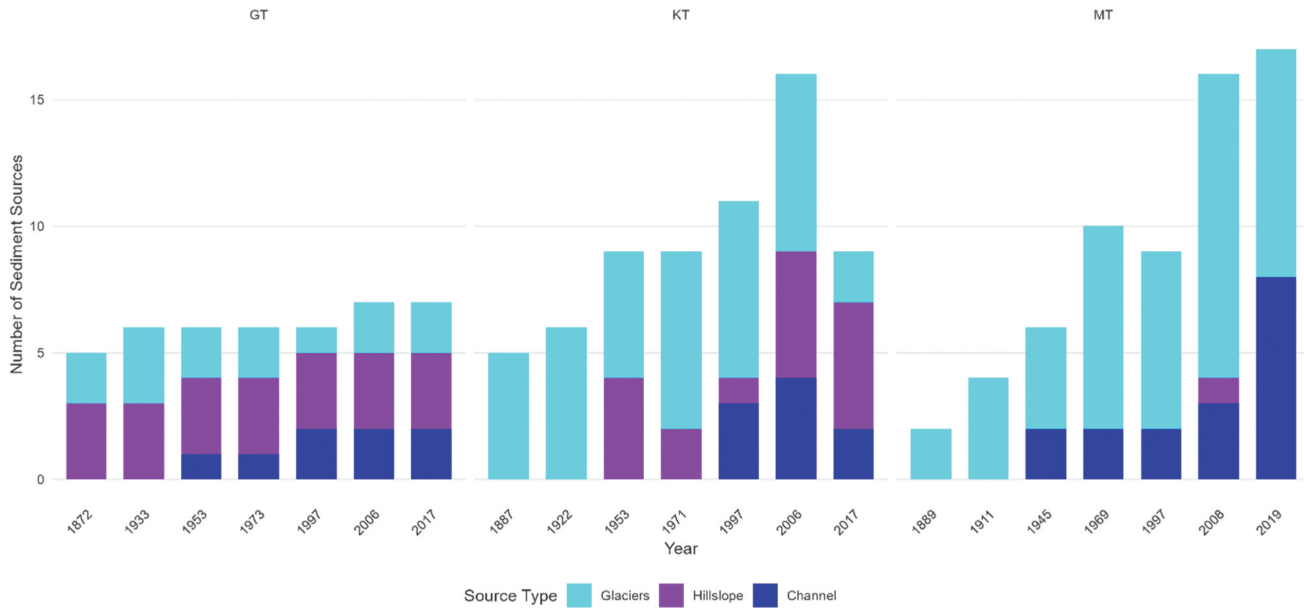

Figure 5. Temporal evolution of the sediment source composition for each study site.

sediment sources (debris flows) are dominant in number, and the overall sum increases only slightly from 5 in 1872 to 7 in 2017. Interpretation of the 1872 and 1933 data is limited by source material constraints: the historical maps do not depict channel sources directly, though the lateral/end moraine above Grastalsee appears to be intact in 1872 and, therefore, most likely did not represent a source. The moraine is subject to substantial erosion from 1997 onwards (>30,000 m^2 between 1997 and 2006), but this is mostly attributable to fluvial erosion and represented as a channel source in Figure 5.

Glacier portals are the most prominent sediment sources in KT, but steep lateral moraines become exposed and active as sources as well from time step 1953 on. The most recent additions here are incisive or laterally eroding reaches, particularly in the area of the so-called "Münchner Abfahrt" (MA). The sharp decline in the last time step is due to the reduction of the number of glacier portals of the Gepatschferner tongue and the complete melting of a glacier snout in the western part of the study site.

In contrast, hillslope processes play a very minor role in the sediment cascade of the Martelltal valley. While some lateral moraines and talus cones show geomorphic activity, they are decoupled from the channel network by extensive ground moraine areas. The exposure of these ground moraines, however, provides material erodible by river streams.

Pathway length

Mean pathway lengths increase across all three study sites over the observation period, though trajectories and rates differ substantially (Figure 6). Pathway length counts the landform transitions (edges) along a source-to-outlet path, not a metric distance. GT exhibits the highest absolute values throughout (11.4 to 16 edges), reflecting its larger spatial extent beyond the proglacial area. Correspondingly, the relative increase in GT (~40 percent) is considerably lower than in KT (~375 percent, from 2 to 9.5 edges) and MT (~267 percent, from 3 to 11 edges), suggesting that GT's sediment cascade network was already more extensively developed at the first time step.

KT and MT show broadly similar magnitudes by the end of the observation period (9.5 and 11 edges, respectively) and both sites display their steepest increases around the turn of the millennium: KT between 1997 and 2006 (6.5 → 10.7), and MT between 1997 and 2008 (8 → 11.3). In KT, the 1997–2006 period shows simultaneous strong increases in both node count and mean pathway length, consistent with longitudinal network expansion as the glacier tongue retreated behind the valley confluence. In MT, node count more than doubles between 1997 and 2008 (29 → 65 nodes), while mean pathway length increases more modestly. This decoupling supports the earlier finding of an increasing edge/node ratio indicating that network growth in MT during this period was not only driven by longitudinal extension of existing pathways, but also by lateral branching of the channel network and lake formation.

Number of pathways

Figure 7 shows the count of pathways between sediment sources and the catchment outlet; solid lines include

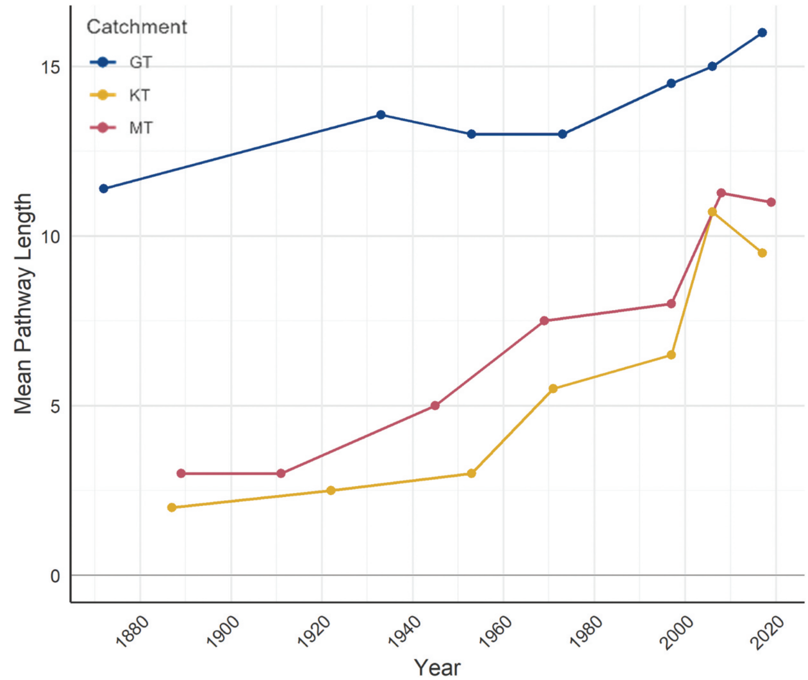

Figure 6. Evolution of mean pathway lengths in the cascade topology graph (number of edges traversed).

lakes as transmitting nodes, dashed lines treat lakes as intercepting barriers.

The GT curve (blue) fluctuates without a clear directional trend in unfiltered pathway count (range 5–9). However, filtered values are consistently lower and show a declining tendency (8 → 3), with the divergence between filtered and unfiltered counts widening over time. By 2017, more than half of all potential pathways (6 unfiltered, 3 filtered) are intercepted by lakes.

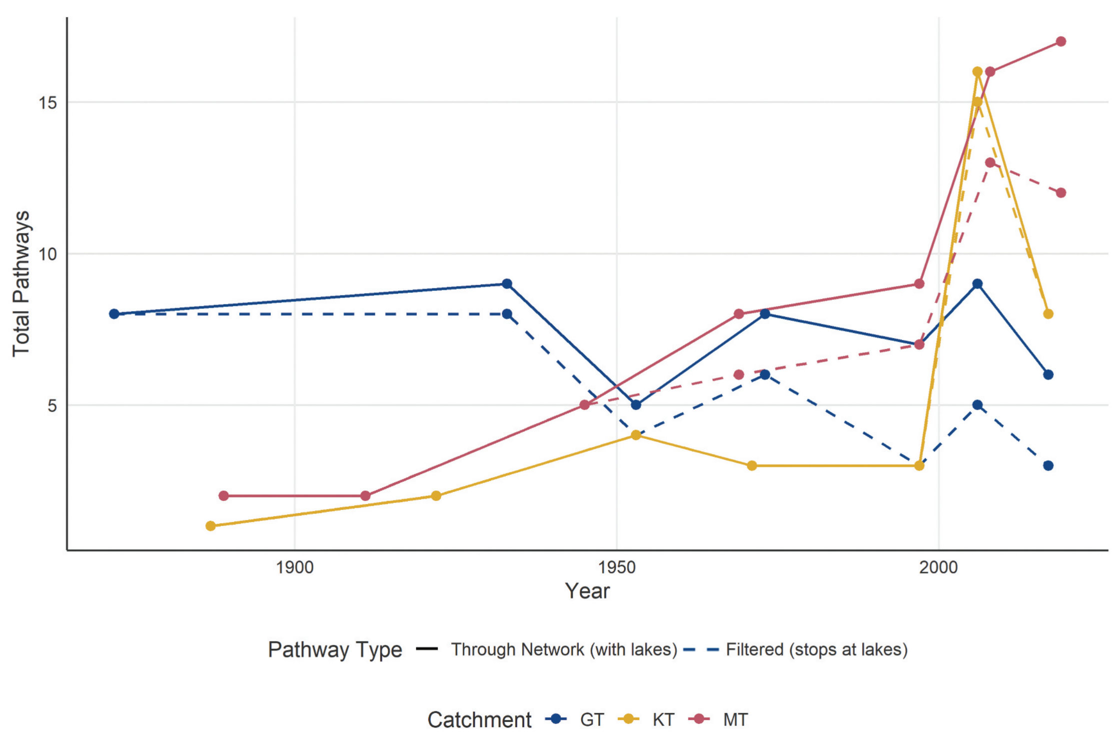

Figure 7. Sediment pathways between all sediment sources and the outlets. Solid lines represent the cascade topology graph including lakes, dashed lines the cascade interrupted by lakes (routing graph).

In KT (orange), filtered and unfiltered values are nearly identical throughout most of the record, indicating that proglacial lakes do not occupy positions that intercept sediment pathways. Pathway counts remain low (1–4) across the first five points in time, reflecting a cascade with minimal branching and consequently high susceptibility to disruption by any single barrier. The sharp increase in 2006 (to 16 pathways) reflects a specific geomorphic configuration: the GZ no longer dammed the valley confluence, coupling several sources from the MA to the main channel network. Additionally, the glacier tongue itself had three portals at this time. This configuration was transient: one snout adjacent to a proglacial lake diminished shortly after (visible in 2009 orthophotos), and another draining into a gorge fell dry following a large flood event in 2012 (Baewert and Morche 2014). By 2017, pathway count had declined to 8, still elevated compared to pre-2006 values.

MT (red) shows the clearest sustained increase in pathway count (2 → 17 unfiltered), consistent with network expansion and increasing sediment source numbers. The divergence between filtered and unfiltered values grows progressively: identical until 1945, differing by 2 in 1969, and reaching a difference of 5 by 2019 (17 unfiltered, 12 filtered). This quantifies the cumulative barrier effect of lake formation, which partially offsets the connectivity gains from network expansion.

Barrier landform positioning

Figure 7 already indicates that the expansion of the sediment cascade due to proglacial area growth can be mitigated by the positioning or emergence of barrier landforms. We also observed that pathway interception by lakes plays a major role in Grastal and Martelltal, but not in Kaunertal. In this section, we first investigate the role of lakes in further detail, then analyze the positioning of braidplains as barriers. Alluvial fans are not considered separately, as the only major alluvial fan (in GT) is positioned adjacent to the Grastalsee and thus does not independently intercept pathways beyond those already blocked by the lake.

Lake emergence and pathway interception

Looking at the number of lakes per study site (Figure 8), it is striking that lake count has increased sharply in the Martell Valley over the last two periods (from 2 to 13), while increasing only modestly in Grastal (from 1 to 3) and fluctuating without clear trend in Kaunertal (range 0–3). For this metric, we did not consider every mapped water-filled depression, but only those with a connection to the channel network.

The high number of proglacial lakes in the Martell Valley is related to the exposure of large ground moraine areas, especially in the Fürkeleferner and Zufallferner forefields (see Figure 9). The lakes in the 2019 map are arranged both parallel and in series, so that only one flow path (the southernmost from Fürkeleferner glacier) passes unintercepted from the glacier to the outlet.

Despite having far fewer lakes than Martelltal (3 versus 13 by 2017), Grastal exhibits the strongest relative barrier effect. Until 2006, this was attributable to a single lake, Grastalsee. At the first time step (1872), neither the original third military survey map nor the 1878 special map of Austria-Hungary depicts a continuous channel

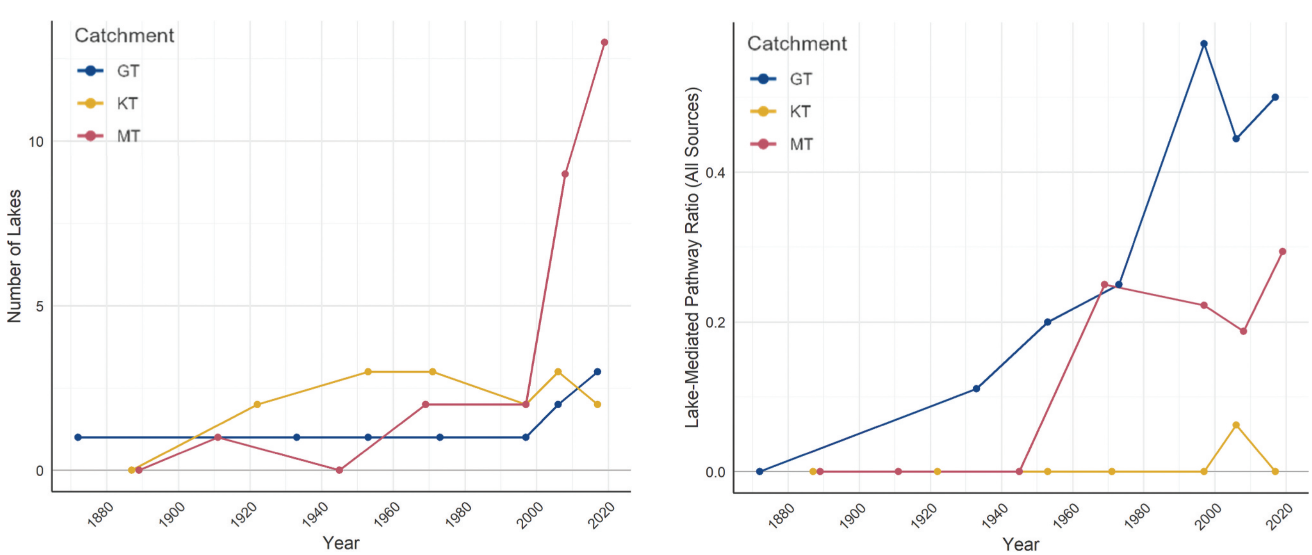

Figure 8. Left panel: Number of lakes per study site and time step. Right panel: Ratio between the number of potential sediment pathways intercepted by lakes and all sediment pathways from sources to the outlet.

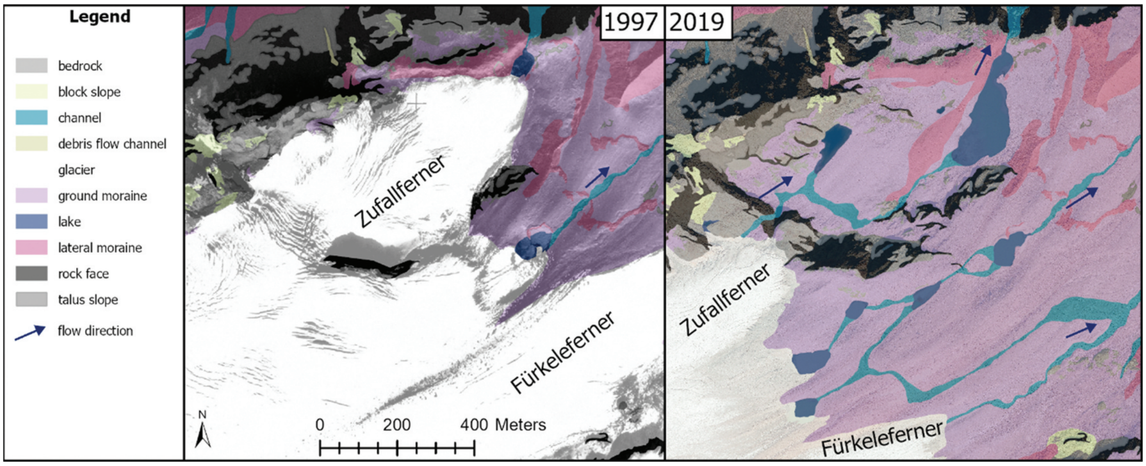

Figure 9. Exemplary sections of the MT geomorphological maps showing the emergence of several proglacial lakes between 1997 and 2019 (with 1997 and 2020 orthophoto in the background, respectively).

from the glacier to Grastalsee, resulting in zero pathway interception, although this interpretation rests on limited source material, with no early photographs available for verification. From 1933 the glacier partially drained into the lake, with the interception ratio rising from 0.11 to 0.57 by 1997. From 1997 onwards, the entire channel network of the proglacial area drains into Grastalsee. The subsequent decrease to 0.44 (2006) reflects transient channel branching in the lower Grastal, at a section where flow paths shifted repeatedly throughout the study period, increasing the total number of pathways outside the proglacial area. A second lake emerged at the glacier margin in 2006, beginning to intercept an additional path by 2017 as the glacier retreated further.

In contrast, we observe a strong increase in lake count in Martell Valley, but its importance expressed as the lake-mediated pathway ratio does not increase proportionally: The pathway ratio reaches 0.25 already in 1969 with only 2 lakes, while 13 lakes in 2019 yield a ratio of only 0.29. This is because many of the newly emerging lakes are arranged in series to already existing ones, affecting pathways that were already intercepted (see Figure 9 for example).

Except for the time step 2006 (ratio of 0.06), the lake-mediated pathway ratio is 0 in Kaunertal, which means that lakes do not intercept sediment pathways, despite 2–3 lakes being present during most of the observation period. This reflects their positioning outside the main sediment cascade.

Braidplain emergence and pathway interception

The number of braidplains increases across all three study sites over the investigation period (Figure 10, left panel). The increase is marginal in Grastal (1 to 2), moderate in Kaunertal (2 to 4), and pronounced in Martelltal (2 to 9). As the lake analysis showed, count alone is insufficient—the position of braidplains within the sediment cascade determines their effect on connectivity. We calculated a braidplain-mediated pathway ratio analogous to the lake analysis (Figure 10, right panel).

In both KT and MT, this ratio equals 1.0 throughout the entire observation period, indicating that all sediment pathways pass through at least one braidplain regardless of network expansion or restructuring. This reflects the position of braidplains at central locations near the catchment outlets. The channel planform is not usually shown explicitly in the historical maps that we used for backdating to the two earliest points in time. In some of the maps, it is indicated by the density of the river branches in a specific area (e.g., the Finsterwalder maps for Kaunertal). We were able to verify the presence of braided reaches in the glacier forefields in the Kaunertal and Martelltal valleys for the earliest dates using photographs (example in Figure 3).

In GT, the braidplain mediation ratio ranges between 0.5 and 0.78, which means that 22–50 percent of pathways bypass braidplains entirely. This can be attributed to debris flow activity on slopes outside the proglacial area that connect directly to the channel network without braidplains along the further pathway.

Event-scale connectivity

The Event Delivery Ratio (EDR) quantifies the proportion of source-derived sediment packages reaching the outlet under a hypothetical hydrometeorological event that simultaneously activates all mapped sources, with each source contributing equally regardless of actual but unknown production rates (section "Event-based

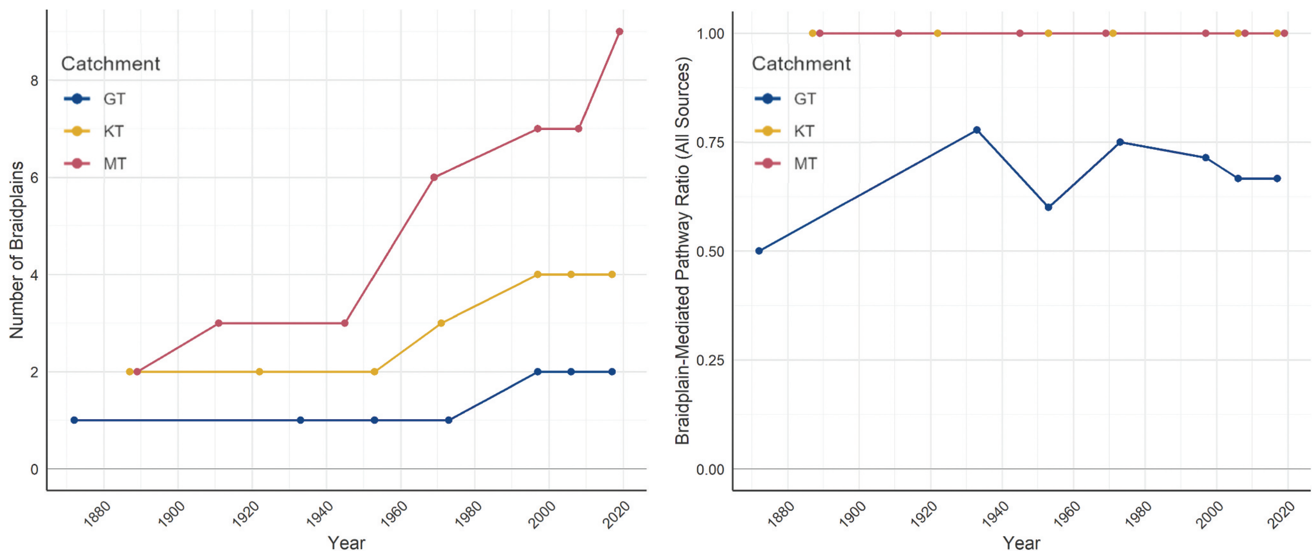

Figure 10. Left panel: Number of braidplains per study site and time step. Right panel: Ratio between the number of potential sediment pathways intercepted by braidplains and all sediment pathways from sources to the outlet.

sediment routing"). Figure 11 shows EDR trajectories for all three catchments (upper panel). The lower panel contextualizes these trajectories by counting source and barrier nodes at each time step, allowing distinction between EDR changes driven by source addition and those driven by barrier expansion.

In the earliest time steps (1887 to 1922), glaciers constituted the only major sediment sources in Kaunertal, yet the EDR remained low (0.10 to 0.17, Figure 11) due to spatial decoupling: several glacier portals at the NG snout drained into the main GZ more than 2 km upvalley from its terminus, causing sediments to be intercepted before reaching the system outlet. The modest EDR increase from 0.10 (1887) to 0.17 (1922) reflects a reduction in the number of these internally decoupled sources as the ice margin geometry simplified. Between 1922 and 1953, several laterally coupled sediment sources became accessible in the forefield of the Gepatschferner tongue. These sources experienced only weak filtering through the "Fernergrieß" (FG) braidplain, driving EDR to 0.20. The subsequent decline through 1971 (0.11) and 1997 (0.09) resulted from two processes: stabilization of some slope sediment sources in the coupled GZ area, while additional sources activated in the decoupled western subcatchment. The sharp EDR increase in 2006 (to 0.20) corresponds to glacier tongue retreating behind the valley confluence, longitudinally coupling meltwater streams and sediment sources from Nördergries and Münchner Abfahrt directly to the outlet. By 2017, EDR reached 0.23, more than double the 1997 value.

The Grastal EDR decreased sharply from 0.90 to 0.60 between 1872 and 1933 and then remained relatively stable (0.60 in 1953) before declining further to 0.40 by 1997. This abrupt early decline corresponds to a shift of the drainage paths upstream of Grastalsee. A glacier melt stream is redirected into the lake passing the LIA terminal moraine and later activated the moraine itself as a source whose sediments are immediately intercepted by the same lake. After 1997, the EDR fluctuated between 0.40 and 0.50 (2006: 0.50; 2017: 0.42). The remaining sediment contributors maintaining these values are deeply incised debris flow channels in the lower valley that bypass the lake and have episodically delivered material to the main channel throughout the study period.

Martelltal exhibited the most substantial increase in accessible sediment sources over the study period (Figure 11 lower panel). However, this signal did not propagate to the outlet under the event scenario: EDR declined from 0.50 (1889) to 0.25 (1911), briefly recovered to 0.29 (1945), and then progressively decreased to 0.10–0.15 through the remainder of the observation period. This attenuation coincides with the comparatively greatest expansion of barrier landforms visible in the lower panel and their strategic positioning at critical network locations (section "Barrier landform positioning").

Discussion

The three study sites experienced substantial glacier retreat and proglacial area expansion over the approximately 150-year observation period, yet their sediment cascade networks evolved along markedly different trajectories. This divergence—despite similar deglaciation forcing and geological setting—raises questions about what controls connectivity evolution in deglaciating systems and whether

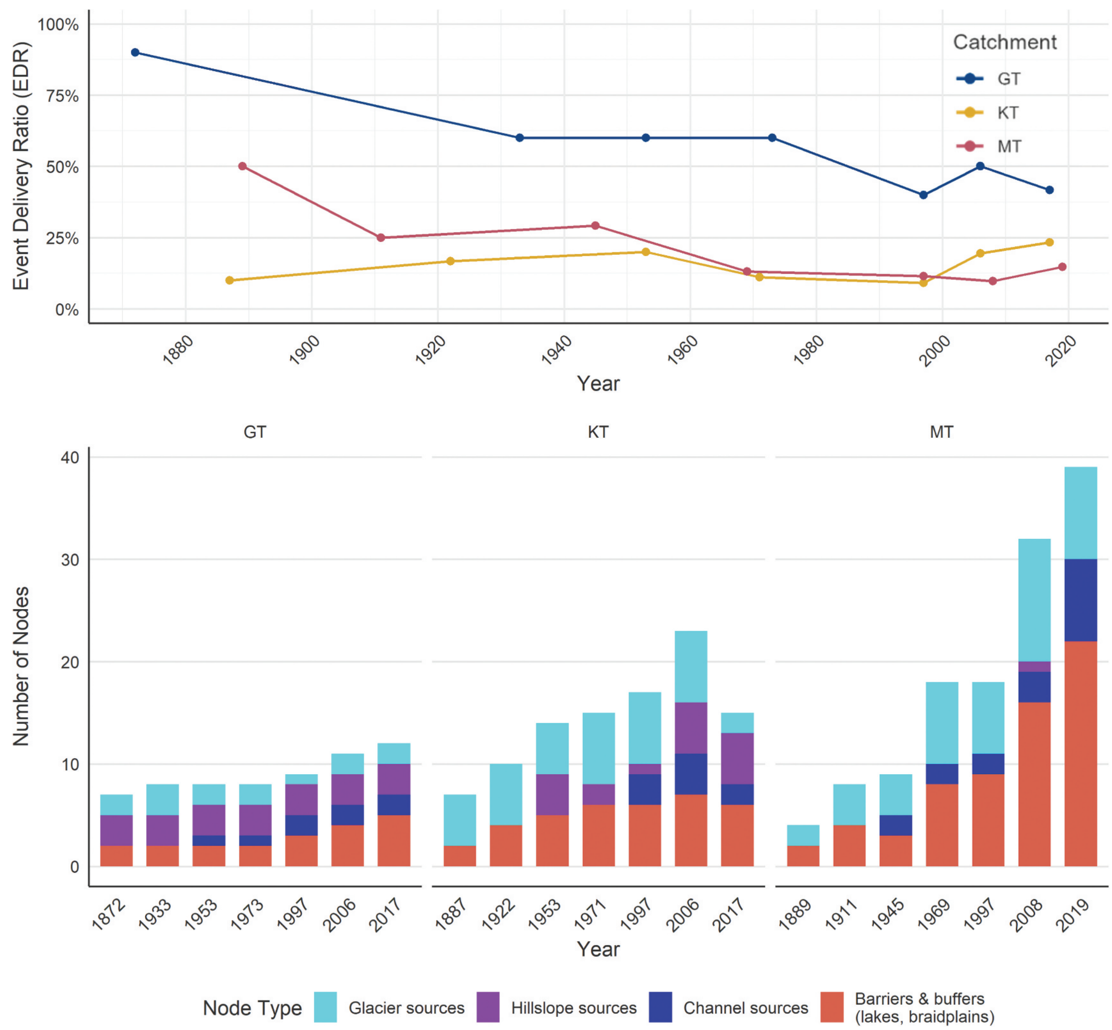

Figure 11. Upper panel: Event Delivery Ratio (EDR) per catchment and time step. Lower panel: composition of contributing (sediment sources by type) and intercepting nodes (lakes and braidplains) in the sediment cascade network at each time step.

generalizable patterns exist. We first interpret the observed structural changes in terms of inherited topography, threshold behavior, and site-specific controls, asking why the catchments diverge rather than converge toward similar configurations. We then examine the effect of the emergence and positioning of barrier landforms—lakes, braidplains, and alluvial fans—on the sediment cascades (Section "Barrier landform control"). Section "Functional connectivity and paraglacial sediment dynamics" combines structural and functional connectivity by evaluating how the observed network changes translate to potential sediment delivery at event timescales, and situates these findings within broader debates on paraglacial sediment dynamics. Given the heterogeneous data sources spanning 150 years, Section "Methodological considerations" explicitly addresses methodological limitations, key assumptions, and their implications for interpreting our results. We conclude with broader implications and directions for future research (Section "Implications and outlook").

Structural evolution and site comparison

The divergent trajectories despite broadly comparable deglaciation forcing indicate that inherited valley topography and glacier geometry, rather than the magnitude of glacier retreat alone, control the mode of network evolution. This spatial heterogeneity is consistent with Kirkbride and Deline (2018), who documented divergent paraglacial trajectories across four Western Alpine cirques and attributed them to local controls—particularly stream-bed material and slope-channel coupling—rather than uniform climate forcing. Our results extend this finding from the cirque to the catchment scale, showing that inherited valley topography controls not only local slope-channel coupling but also the system-scale network architecture through which sediment must travel.

Paraglacial conceptual models describe the evolution of sediment supply from glacially conditioned sources during deglaciation, typically as an exponential decline driven by progressive source exhaustion or stabilization (Ballantyne 2002). More recent frameworks recognize that sediment delivery is also modulated by evolving connectivity, with proglacial lakes, moraines and alluvial fans interrupting sediment transfer and the reorganization of source-to-sink pathways altering delivery efficiency (Zhang et al. 2022). Our results empirically quantify this structural dimension: the network of landforms through which mobilized sediment must travel reorganizes non-monotonically during deglaciation, and whether sediment released from sources reaches the catchment outlet depends on where barriers and pathways emerge relative to inherited topography. Sediment supply and source activity at our study sites have been investigated at the scale of individual landforms and processes (Betz-Nutz et al. 2023; Piermattei et al. 2023; Rom et al. 2023a; Altmann et al. 2024). Holding source activity constant in the graph framework isolates the filtering effect of network structure from the effects of variable supply, allowing the structural dimension of paraglacial adjustment to be compared directly across catchments and time steps. Sensitivity—the capacity of landforms and systems to adjust morphologically under forcing—and connectivity are fundamentally linked controls that together govern a system's response to disturbance (Fryirs 2017; Lisenby, Croke, and Fryirs 2018). Reconstructing the connectivity axis at catchment scale, therefore, complements the landform- and process-scale work on source activity at our sites.

In Kaunertal, the dominant control was the position of the Gepatschferner tongue relative to the valley confluence. While the glacier blocked this junction, the Münchner Abfahrt and Nördergries subcatchments remained structurally decoupled from the trunk channel. The retreat of the tongue behind the confluence between 1997 and 2006 triggered a threshold-like reorganization that integrated previously isolated subcatchments into a single connected cascade. This stepwise transition demonstrates that glacier retreat can produce topological transitions where small additional retreat causes disproportionate structural change. The laterally confined valley walls constrain network development to longitudinal extension, so that subsequent retreat produces a lengthening but topologically simple cascade. Rising mean pathway lengths are functionally relevant because each additional landform transition constitutes a potential buffering or filtering step between source and outlet, so that longitudinal network growth alone increases the structural filtering potential of the cascade.

Martelltal followed a different trajectory despite similar deglaciation forcing: sustained lateral network expansion driven by the exposure of extensive ground moraine areas where multiple proglacial lakes and branching channel networks formed. This non-monotonic development mirrors the regional glacier activity record, with readvances in the 1920s, stronger retreat between 1930 and 1964, and another readvance between 1965 and 1985 (Kuhn, Schlosser, and Span 1997). The increasing edge/node ratio, exceeding 1.0 by the most recent time step, indicates a shift from a simple cascade toward a more complex network characterized by multiple alternative pathways. However, this expansion simultaneously introduced new barriers, so that connectivity-enhancing and connectivity-reducing processes operated concurrently.

Grastal presents a case where Grastalsee, positioned directly downstream of the LIA terminal moraine, progressively intercepted an increasing share of sediment pathways as glacier meltwater drainage shifted into the lake. This proximity means that changes in proglacial drainage configuration at the glacier margin directly control whether sediment reaches or bypasses the lake. This contrasts with Kaunertal and Martelltal, where downstream reaches outside the LIA boundary function as transport pathways without further topologically significant barriers before their respective reservoirs. Only in Grastal does the interaction between barrier positioning outside the LIA boundary and drainage changes within it exert first-order control on system connectivity, a configuration that justifies extending the analysis beyond the proglacial area. These three contrasting modes reflect the concept of topographic inheritance (Carrivick and Heckmann 2017): inherited valley confinement, substrate, and glacier-bed morphology predetermine the mode and direction of network evolution.

The steepest increases in pathway metrics cluster around the turn of the millennium in both Kaunertal (1997–2006) and Martelltal (1997–2008), coinciding with accelerated glacier retreat during this period (Zemp et al. 2015; Figure 4). However, the temporal coincidence should not be read as a simple area-response relationship. In Kaunertal, the inflection reflects a specific topographic threshold rather than a proportional response to retreat rate. In Martelltal, the rapid network expansion reflects terrain predisposed to lake formation and channel branching by glacier bed morphology. The slight node-count decline in the final time step at all three sites reflects glaciers retreating behind drainage divides, so that previously existing drainage paths disappear.

Barrier landform control

Section "Structural evolution and site comparison" established that barrier emergence and positioning drive divergent connectivity trajectories. Here we examine the mechanisms by which different barrier types (following the terminology of Fryirs et al. 2007a) control sediment transfer and how their effectiveness relates to network position rather than abundance. Lakes function as complete barriers to coarse sediment (Bogen, Xu, and Kennie 2015), but their system-scale impact depends critically on topological position.

In Martelltal, lake count increased sharply after 1997 (Figure 8), yet the lake-pathway ratio increased only modestly. Many new lakes formed in series along pathways already interrupted by existing lakes, yielding diminishing marginal effects on structural connectivity. This mirrors the more general pattern that, where retreating glaciers expose overdeepenings arranged as a cascade, the most proximal basins intercept most of the incoming sediment while those farther downstream add progressively less (Veh et al. 2026). The Martelltal trajectory illustrates that topological importance does not necessarily scale with barrier count: as the proglacial area expanded and lakes proliferated, additional lakes contributed marginally to system-scale interception. In Kaunertal, the 2–3 lakes present during most of the observation period remained peripheral to the main sediment cascade, contributing negligibly to pathway interception. The three sites together demonstrate that lake inventories alone cannot predict connectivity effects without accounting for network topology.

Lake lifespans also differ systematically among sites. The Martelltal proglacial lakes are small, show signs of rapid sedimentation, suggesting they will act as effective sediment traps on the order of years to decades. Grastalsee, by contrast, is positioned to function as a sediment trap over much longer timescales: bathymetric comparison between 1981 and 2024 indicates ca. 50,000 m^3 of sediment accumulation over 43 years, with ~490,000 m^3 of remaining capacity, suggesting centuries of continued effectiveness (Baumgartner 2025).

Once effective barrier configurations become established—as in Grastal after the drainage shift or Martelltal with the emergence of proglacial lakes—subsequent changes in source availability have limited effect on system-scale connectivity. Turley and Hassan (2023) documented similar structural persistence at Mount Rainier, where inherited glacial macroforms controlled spatial patterns of sediment transfer over millennial timescales. Their finding that disconnectivity represents the dominant state of natural sediment cascades resonates with our observation that barrier configurations can constrain connectivity evolution regardless of continued deglaciation and source expansion.

Unlike lakes, braidplains attenuate rather than terminate coarse sediment flux, alternating between net erosion and aggradation phases over decadal timescales (Mancini et al. 2023; Piermattei et al. 2023). Their position determines how much they attenuate the coarse sediment reaching the outlet: in Kaunertal and Martelltal, braidplains occupy central, near-outlet positions that every source-to-outlet pathway must traverse, so all coarse sediment delivered to the outlet has passed through at least one attenuating reach; in Grastal, debris-flow channels couple hillslopes directly to the main channel and bypass the proglacial braidplain, so part of the coarse sediment load reaches the outlet without this attenuation.

The only alluvial fan mapped as a distinct barrier landform lies between the LIA moraine and Grastalsee in Grastal; due to its position immediately upstream of the lake, it does not independently intercept pathways beyond those already blocked by Grastalsee. It nonetheless illustrates that serial barrier arrangements can extend the effective lifespan of downstream barriers by reducing their sediment load (Himmelstoss et al. 2024).

Functional connectivity and paraglacial sediment dynamics

The preceding sections examined structural connectivity —the configuration of pathways and barriers—which evolves over decades to centuries. A central challenge in connectivity research is linking these structural configurations to functional connectivity: actual sediment transfer under specific forcing conditions (Wainwright et al. 2011; Wohl et al. 2019). The EDR modeling provides a bridge by simulating the filtering of sediment unit delivery by network structure during hypothetical high-magnitude events that activate all mapped sources susceptible to hydro-meteorological forcing. The filtering coefficients were derived from rare observation data on landform sediment delivery ratios at event scale (Himmelstoss et al. 2024).

Because every sediment pathway in our analysis begins at a mapped source, the composition of those sources and the forcing that activates them set what the network subsequently filters. Dominant sediment source types differ markedly among sites (Figure 5), with consequences for which forcings dominate system response. Glacier portals and actively eroding lateral moraines dominate in Kaunertal, consistent with Hilger et al.'s (2019) sediment budget identifying the Gepatschferner and fluvial erosion as principal contributors. In Grastal, hillslope debris flows constitute the primary coupled sources besides the breached LIA moraine as the most active proglacial source. In Martelltal, channel sources predominate while hillslope-channel coupling is limited by the extensive low-gradient moraine surfaces that buffer lateral inputs. These compositional differences mean that debris flow-dominated systems like Grastal respond primarily to precipitation extremes (Himmelstoss et al. 2024, 2025), whereas glacier-dominated systems like Kaunertal respond more directly to thermal forcing and meltwater dynamics (Comiti et al. 2019; Morche et al. 2019). The EDR's high-magnitude-event framing applies most directly to systems where the dominant sources can plausibly be activated within a single event; site-specific differences in source composition, therefore, set bounds on how literally EDR trajectories should be read across catchments.

Grastal and Martelltal both show sustained EDR decline over the observation period, but via different mechanisms: In Grastal, the decline is driven by progressive redirection of proglacial drainage into Grastalsee; in Martelltal, it is driven by the emergence of new barriers (lakes and braidplains) that reduce the proportion of sediment units reaching the outlet (Sections "Barrier landform positioning" and "Event-scale connectivity"). Kaunertal takes a different trajectory. The 1997–2006 topology shift coupled previously isolated Münchner Abfahrt and Nördergries sources directly to the outlet. The values remain modest, and the rise is driven by a single topological transition rather than a sustained trend, but the direction contrasts with the other two sites.

Our approach builds on established frameworks for catchment-scale connectivity analysis. The buffer/barrier/blanket framework (Fryirs et al. 2007a) and the effective catchment area concept (Fryirs et al. 2007b; Turley and Hassan 2023) formalize how landforms reduce the area actively contributing sediment to a catchment outlet. Our approach is conceptually aligned with these frameworks: source mapping, pathway counts, and pathway ratios identify which sources become or remain connected and if these connections are interrupted. The graph-based approach extends this logic in three ways. First, the EDR allows partial filtering rather than binary connected/disconnected classification, necessary because braidplains and alluvial fans attenuate rather than terminate coarse sediment flux (Mancini et al. 2023; Piermattei et al. 2023). Second, it makes the positional dependence of barriers explicit and quantifiable, enabling comparison across systems where landform inventories alone would suggest misleading equivalences. Third, the approach enables structural connectivity reconstruction over the full post-LIA period, a temporal reach beyond what DEM-based approaches like ECA can provide. Because graph metrics are computed consistently across all 21 maps, connectivity states at different time steps are directly comparable without requiring subjective expert judgment for each map individually (Heckmann, Schwanghart, and Phillips 2015).

Lane et al. (2017) proposed that proglacial systems may shift toward increasing event-dependence as structural barriers accumulate, reducing background sediment transfer and concentrating delivery into high-magnitude episodes. Buter et al. (2022) reached a similar conclusion for the neighboring Sulden and Trafoi subcatchments in the Ortler Alps, attributing differences in functional connectivity to contrasting glacier-channel coupling: well-connected Sulden was predicted to transfer sediment relatively continuously, while Trafoi was predicted to become increasingly event-dependent. Our results for Grastal and Martelltal are consistent with the second trajectory: pronounced source expansion was accompanied by barrier emergence that offset the connectivity gains. Mancini and Lane (2020) documented a similar pattern at hillslope-forefield scale, where gully erosion enhanced lateral coupling, but the eroded sediment accumulated on alluvial fans that buffered further transfer. Deglaciation thus simultaneously expands the area potentially supplying sediment—as glaciers expose new ground moraine and proglacial slopes—and the inventory of landforms that intercept it. The effective sediment-contributing area reflects the balance between these opposing processes.

Kaunertal presents a partial counterpoint. Piermattei et al. (2023) suggested the trend toward negative sediment balance in the Fagge River may reflect not only increasing transport capacity but also declining sediment supply from exhaustion of readily erodible glacigenic stores. Similar dynamics—either through supply exhaustion or through progressive armoring of exposed sediment that reduces its transportability—have been documented in other Alpine catchments (Lane et al. 2017; Delaney et al. 2018). Our analysis indicates, however, that structural connectivity rose from 1997 onward. Suspended sediment monitoring since 2008 at the Gepatschalm gauging station shows that the largest transport events are associated with incision and lateral erosion in the previously decoupled Münchner Abfahrt and Nördergries reaches, suggesting the structural change has functional consequences. These observations are not necessarily contradictory. A system can simultaneously experience declining total sediment availability (as sources become less active or stores become exhausted) and increasing connectivity (as barriers disappear or drainage reorganizes). The net effect on sediment export depends on which process dominates—a question that cannot be resolved from structural analysis alone but requires coupling with multi-temporal sediment budget or continuous yield data.

The Kaunertal case also illustrates that the current trend may be transient. Ice-thickness models predict several glacier bed overdeepenings (>10,000 m^2) at mid-to-upper elevations on the Gepatschferner (Otto et al. 2022). If these become lakes upon further glacier retreat, Kaunertal's connectivity trajectory could reverse, shifting from the current increase toward the declining pattern observed in Martelltal and Grastal. Structural connectivity analysis thus provides not only retrospective understanding but also a framework for anticipating future system states given projected deglaciation.

Methodological considerations

Integrating different data sources spanning 150 years raises the question whether apparent network changes reflect real system evolution or improvements in data quality over time. Two aspects of the approach mitigate this concern: First, the graph operates on landform units rather than raster cells: pixel-level flow is routed and summed into connections between mapped landforms, so pathway counts depend on landform boundaries and their connectivity, not on pixel-level DEM or imagery resolution (section "Graph creation"). This makes the approach less sensitive to resolution differences than pixel-based methods and supports comparison across historical maps, SfM-derived products, and ALS DEMs. Second, the most pronounced network changes correspond to large, unambiguous features (lakes, glaciers) identifiable across all data generations. Contemporary photographs support the presence of important fluvial features like braided reaches at the earliest dates. Resolution differences may still blur fine-scale detail in the earliest maps but cannot plausibly generate this magnitude of restructuring.

For the two earliest time steps, DoD-based sediment source identification was not possible. We assumed that hillslope sources mapped as active in subsequent periods were also active earlier, provided they were not glacier-covered and adjacent channels occupied similar positions. This assumption is supported by studies showing stable or declining lateral moraine erosion rates (Betz-Nutz et al. 2023; Altmann et al. 2024) and the absence of a clear temporal trend in debris flow activity (Rom et al. 2023a, 2023b) at our study sites, but it cannot be directly verified.

The EDR model's filter coefficients derive from a single event in Grastal (Himmelstoss et al. 2024). Braidplain bedload throughput depends on the supply-to-capacity ratio and on valley form (width, slope), switching between deposition- and transfer-dominated regimes (Mancini et al. 2025). Realistic coefficients likely vary with event magnitude, antecedent morphology, and glacier melt intensity, as well as systematically between and within catchments—variability the current model does not capture and the available data cannot constrain across our sites and time steps. We therefore hold the coefficients fixed and interpret EDR values as indices for comparing network configurations under a controlled set of assumptions, not as predicted delivery ratios for any specific event.

We excluded processes contributing marginally to sediment budgets of our study sites (periglacial creep, low-magnitude rockfall, avalanches; Vehling et al. 2017; Hilger and Beylich 2019) and did not incorporate vertical connectivity factors (vegetation, armoring) that could be added as node attributes where data exist. Our algorithm conservatively removes fluvial edges routing sediment into glaciers, potentially underestimating connectivity where subglacial transport is efficient.

The graph-based approach occupies a methodological niche relative to alternatives (Shi et al. 2025). The Index of Connectivity (Cavalli et al. 2013) offers continuous spatial coverage and predictive power for specific processes (Steger et al. 2022; Himmelstoss et al. 2025; Tsyplenkov et al. 2025), but does not represent landform topology or distinguish barrier types, and its robustness to data quality differences across historical SfM-derived and modern ALS-DEMs remains untested. Numerical models like CASCADE (Schmitt, Bizzi, and Castelletti 2016; Tangi et al. 2022) or CAESAR-Lisflood (Coulthard and Van De Wiel 2017) simulate transport dynamics but require input data rarely available for century-scale analysis. Graph-based analysis explicitly represents network topology and functional roles, accommodates heterogeneous data through landform aggregation, and scales across catchments and time period, with the trade-off of abstracting within-landform processes.

Implications and outlook

This study shows that graph theory supports structural connectivity analysis over the post-LIA period, integrating historical maps, SfM products, and ALS DEMs within a single framework. Across our three catchments, connectivity evolution depends not only on the magnitude of glacier retreat but on where new sources and barriers emerge relative to inherited topography. Graph analysis makes this site-specific topological control explicit, quantifiable, and comparable between catchments, complementing process-based conceptual models with a network-structural assessment.

The demonstration that barrier positioning outweighs barrier abundance has practical implications for connectivity assessment. Proglacial lake inventories are insufficient proxies for catchment connectivity without topological context. Graph-based screening could identify catchments where few barriers occupy critical network positions versus those where numerous barriers have limited system-scale effect. Beyond the applications presented here, the graph framework opens several avenues for extension:

Attribute enrichment

The current representation treats landforms as functionally homogeneous. Node attributes such as vegetation cover, permafrost distribution, or sediment thickness could refine connectivity estimates by indicating stabilization potential or susceptibility to future activation. Vegetation succession, for instance, progressively stabilizes slopes and channels and reduces sediment availability during paraglacial adjustment (Klaar et al. 2015; Eichel 2019). Edge attributes, like stream gradient as a proxy for transport competence, or DoD-derived flux estimates where available, could differentiate high-efficiency transport links from storage-prone reaches. Such enrichment would bridge the current gap between structural topology and process intensity.

Multi-fraction routing

The EDR model as formulated here targets bedload: lakes are treated as complete sinks, braidplains and alluvial fans as partial bedload filters. Suspended-load cascades would require different storage relationships and filter coefficients, reflecting the contrasting retention dynamics of fine sediment across landform types (Mao et al. 2019; Mancini et al. 2023). Parallel routing of multiple grain-size fractions would extend the framework to the full sediment continuum.

Scaling

The networks analyzed here comprise tens to hundreds of nodes, a scale amenable to direct interpretation. Regional comparisons or analysis of larger systems may benefit from hierarchical approaches where catchment-scale graphs serve as nodes in regional networks. Conversely, landforms identified as topologically critical could be expanded into higher-resolution subgraphs for process-based analysis, as demonstrated for braided river reaches by Connor-Streich et al. (2018). Systematic application across more catchments with varying confinement, aspect, glacier type, and lithology would test whether the divergent patterns observed here generalize or reflect site-specific conditions.

Cascading hazard assessment

The landform-based graph structure enables detection of topological configurations associated with process chains. Lakes dammed by moraines, steep rock slopes above lakes or glaciers, and debris-covered ice in contact with growing lakes represent recognizable cascade architectures. A historical ice-dammed lake at Zufallferner in Martelltal, which produced multiple glacial lake outburst floods (GLOFs) in the late 19th century (Finsterwalder 1890), exemplifies such configurations. Graph-based screening for such recurring topological configurations (Ekkirala and Ramesh 2026) could support systematic identification of emerging cascade architectures as proglacial lakes proliferate under continued warming (Zheng et al. 2021; Zhang, Wang, and An 2024).

Coupling with sediment budgets

Linking the structural trajectories documented here with measured sediment export remains essential for determining the functional consequences of structural changes for sediment delivery. Both Kaunertal and Martelltal drain into reservoirs with similar catchment areas (~61–62 km^2): for Kaunertal, a pre-impoundment DEM combined with a 2015 drainage survey yields a cumulative sediment budget since dam construction (Schöber and Hofer 2018), and ongoing repeat surveys will enable tracking of recent trends. Comparing decadal-scale yields against the contrasting structural trajectories documented here would test whether the structural framework predicts functional divergence, or whether factors not captured by topology—e.g., sediment availability, transport capacity, event sequencing—dominate export variability.

Conclusion

This study demonstrates that graph theory provides a framework for quantifying the structural evolution of sediment connectivity in deglaciating Alpine catchments across decadal to centennial timescales. Using geomorphological landforms as fundamental graph units rather than grid cells accommodates heterogeneous historical data sources—maps, terrestrial photographs, SfM-derived products, and ALS-derived DEMs—within a single analytical framework, enabling quantitative comparison across study sites and time periods.

The three catchments (Grastal, Kaunertal, and Martelltal) experienced substantial deglaciation and sediment source expansion yet evolved along markedly different structural trajectories, driven by site-specific interactions between deglaciation and inherited topography. In Kaunertal, connectivity increased when the glacier retreated behind a valley confluence, coupling previously isolated subcatchments to the outlet. In Martelltal, pronounced source expansion was offset by the proliferation of proglacial lakes and braidplains. In Grastal, progressive redirection of glacier meltwater into Grastalsee constrained connectivity regardless of changes further upstream. Event-based routing mirrored this divergence: simulated sediment delivery increased in Kaunertal while declining in both Grastal and Martelltal, indicating that network restructuring can outweigh source expansion in setting potential sediment delivery. The topological position of barrier landforms within the network, rather than their abundance, determined system-scale filtering effectiveness.

Structural changes were non-linear and often episodic. Threshold-like transitions occurred at Kaunertal and Grastal near the turn of the millennium, when retreating glaciers crossed topologically significant boundaries. Martelltal's decline was instead progressive, driven by incremental barrier accumulation. These contrasting temporal patterns indicate that connectivity responses depend on the spatial arrangement of emerging landforms relative to the inherited cascade, not on cumulative glacier loss alone.

Linking structural to functional connectivity—actual sediment transfer under specific forcing—remains a central challenge, and comparison with independently measured sediment export (for example, from reservoir bathymetry) is needed to test whether the divergent trajectories documented here translate into measurable differences in catchment yield. As proglacial systems continue to expand under ongoing climate warming, understanding how their structural connectivity evolves will be essential for predicting downstream sediment delivery, managing reservoir sedimentation, and anticipating cascading hazards. The divergent trajectories documented here caution against assuming uniform connectivity responses to glacier retreat across Alpine catchments.

Acknowledgments

We thank the reviewers for their careful and engaged reading of the manuscript; their constructive comments substantially improved its clarity and rigour.

Author contributions

CRediT: **Toni Himmelstoss:** Conceptualization, Formal analysis, Investigation, Methodology, Validation, Visualization, Writing – original draft, Writing – review & editing; **Lena Bartram:** Investigation, Methodology; **Florian Haas:** Funding acquisition, Project administration, Resources, Supervision; **Michael Becht:** Funding acquisition, Project administration, Resources, Supervision; **Tobias Heckmann:** Conceptualization, Funding acquisition, Methodology, Project administration, Resources, Supervision, Writing – review & editing.

Disclosure statement

No potential conflict of interest was reported by the author(s).

Generative AI was used for.

- Language improvement (Claude Opus 4.5–4.8)
- Coding assistance (Claude Sonnet 4.5–5)

The use of our data for training and improving the AI models was excluded, and the authors reviewed all outputs of the Generative AI tools.

Funding

This work was supported by the German Research Foundation (Deutsche Forschungsgemeinschaft) under Grant FOR 2793, the Austrian Science Fund under Grant 4062-N29, and the Autonomous province of South Tyrol, Grant IT-DFG 781607.

ORCID

Toni Himmelstoss http://orcid.org/0009-0003-7943-3780
Florian Haas http://orcid.org/0000-0002-4874-2527
Michael Becht http://orcid.org/0000-0001-9214-8165
Tobias Heckmann http://orcid.org/0000-0002-1495-4214

References

Altmann, M., F. Haas, T. Heckmann, F. Liébault, and M. Becht. 2021. Modelling of sediment supply from torrent catchments in the Western Alps using the sediment contributing area (SCA) approach. *Earth Surface Processes and Landforms* 46, no. 5: 889–906. doi:10.1002/esp.5046.

Altmann, M., M. Pfeiffer, F. Haas, J. Rom, F. Fleischer, T. Heckmann, L. Piermattei, et al. 2024. Long-term monitoring (1953–2019) of geomorphologically active sections of Little Ice Age lateral moraines in the context of changing meteorological conditions. *Earth Surface Dynamics* 12, no. 1: 399–431. doi:10.5194/esurf-12-399-2024.

Baewert, H., and D. Morche. 2014. Coarse sediment dynamics in a proglacial fluvial system (Fagge River, Tyrol). *Geomorphology* 218: 88–97. doi:10.1016/j.geomorph.2013.10.021.

Ballantyne, C.K. 2002. A general model of paraglacial landscape response. *The Holocene* 12, no. 3: 371–6. doi:10.1191/0959683602hl553fa.

Baumgartner, M.K. 2025. *Bathymetrische Analyse eines proglazialen Sees im Grastal*. Eichstätt: Tirol, Katholische Universität Eichstätt-Ingolstadt.

Bayens, M., A. Ballu, B. Ruols, and S.N. Lane. 2025. Microscale topographic controls on functional hillslope-to-stream connectivity in rapidly deglaciating terrain. *Geomorphology* 486: 109902. doi:10.1016/j.geomorph.2025.109902.

Becht, M. 1995. *Untersuchungen zur aktuellen Reliefentwicklung in alpinen Einzugsgebieten: Mit 40 Tabellen* . Geobuch-Verl: München.

Bennett, G.L., D.J.A. Evans, P. Carbonneau, and D.R. Twigg. 2010. Evolution of a debris-charged glacier landsystem, Kvíárjökull, Iceland. *Journal of Maps* 6, no. 1: 40–67. doi:10.4113/jom.2010.1114.

Betz-Nutz, S., T. Heckmann, F. Haas, and M. Becht. 2023. Development of the morphodynamics on Little Ice Age lateral moraines in 10 glacier forefields of the Eastern Alps since the 1950s. *Earth Surface Dynamics* 11, no. 2: 203–26. doi:10.5194/esurf-11-203-2023.

Bogen, J., M. Xu, and P. Kennie. 2015. The impact of proglacial lakes on downstream sediment delivery in Norway. *Earth Surface Processes and Landforms* 40, no. 7: 942–52. doi:10.1002/esp.3669.

Bollati, I.M., M. Cavalli, A. Masseroli, C. Viani, F. Moraschina, and M. Pelfini. 2024. Thematic mapping for sediment cascade analysis in small mountain catchments – The case of the Buscagna valley (Lepontine Alps). *Geomorphology* 446: 109001. doi:10.1016/j.geomorph.2023.109001.

Buter, A., T. Heckmann, L. Filisetti, S. Savi, L. Mao, B. Gems, and F. Comiti. 2022. Effects of catchment characteristics and hydro-meteorological scenarios on sediment connectivity in glacierised catchments. *Geomorphology* 402: 108128. doi:10.1016/j.geomorph.2022.108128.

Buter, A., A. Spitzer, F. Comiti, and T. Heckmann. 2020. Geomorphology of the Sulden River basin (Italian Alps) with a focus on sediment connectivity. *Journal of Maps* 16, no. 2: 890–901. doi:10.1080/17445647.2020.1841036.

Carrivick, J.L., and T. Heckmann. 2017. Short-term geomorphological evolution of proglacial systems. *Geomorphology* 287: 3–28. doi:10.1016/j.geomorph.2017.01.037.

Carrivick, J.L., and F.S. Tweed. 2021. Deglaciation controls on sediment yield: Towards capturing spatio-temporal variability. *Earth-Science Reviews* 221: 103809. doi:10.1016/j.earscirev.2021.103809.

Cavalli, M., T. Heckmann, and L. Marchi. 2019. Sediment Connectivity in Proglacial Areas. In *Geomorphology of Proglacial Systems*, T. Heckmann and D. Morche, eds. Cham: Springer International Publishing, 271–87.

Cavalli, M., S. Trevisani, F. Comiti, and L. Marchi. 2013. Geomorphometric assessment of spatial sediment connectivity in small Alpine catchments. *Geomorphology* 188: 31–41. doi:10.1016/j.geomorph.2012.05.007.

Comiti, F., L. Mao, D. Penna, A. Dell'agnese, M. Engel, S. Rathburn, and M. Cavalli. 2019. Glacier melt runoff controls bedload transport in Alpine catchments. *Earth and Planetary Science Letters* 520: 77–86. doi:10.1016/j.epsl.2019.05.031.

Connor-Streich, G., A.J. Henshaw, J. Brasington, W. Bertoldi, and G.L. Harvey. 2018. Let's get connected: A new graph theory-based approach and toolbox for understanding braided river morphodynamics. *WIREs Water* 5, no. 5: e1296. doi:10.1002/wat2.1296.

Cossart, É., and M. Fressard. 2017. Assessment of structural sediment connectivity within catchments: Insights from graph theory. *Earth Surface Dynamics* 5, no. 2: 253–68. doi:10.5194/esurf-5-253-2017.

Coulthard, T.J., and M.J. Van De Wiel. 2017. Modelling long term basin scale sediment connectivity, driven by spatial land use changes. *Geomorphology* 277: 265–81. doi:10.1016/j.geomorph.2016.05.027.

Csardi, G., and T. Nepusz. 2006. The igraph software package for complex network research. *Complex Systems* 1695: 1–9.

Delaney, I., A. Bauder, M. Huss, and Y. Weidmann. 2018. Proglacial erosion rates and processes in a glacierized catchment in the Swiss Alps. *Earth Surface Processes and Landforms* 43, no. 4: 765–78. doi:10.1002/esp.4239.

Eichel, J. 2019. Vegetation Succession and Biogeomorphic Interactions in Glacier Forelands. In *Geomorphology of Proglacial Systems*, T. Heckmann and D. Morche, ed. Cham: Springer International Publishing, 327–49.

Ekkirala, H.C., and M.V. Ramesh. 2026. Spatiotemporal assessment of multi hazard risk using graph based analysis for case studies in India. *Scientific Reports* 16, no. 1: 5837. doi:10.1038/s41598-026-35925-4.

Fan, X., F. Hofmeister, B. Schaefli, and G. Chiogna. 2025. *Physics-based simulation of hydrological processes in a high-elevation glaciated environment focusing on groundwater*. Munich: EGUsphere. doi: 10.5194/egusphere-2025-1500.

Finsterwalder, S. 1890. Die Gletscherausbrüche des Martell-Thales. *Zeitschrift Des Deutschen Und Oesterreichischen Alpenvereins* 21: 21–34.

Fressard, M., and E. Cossart. 2019. A graph theory tool for assessing structural sediment connectivity: Development and application in the Mercurey vineyards (France). *The Science of the Total Environment* 651: 2566–84. doi:10.1016/j.scitotenv.2018.10.158.

Fryirs, K.A. 2017. River sensitivity: A lost foundation concept in fluvial geomorphology. *Earth Surface Processes and Landforms* 42, no. 1: 55–70. doi:10.1002/esp.3940.

Fryirs, K.A., G.J. Brierley, N.J. Preston, and M. Kasai. 2007a. Buffers, barriers and blankets: The (dis)connectivity of catchment-scale sediment cascades. *Catena* 70, no. 1: 49–67. doi:10.1016/j.catena.2006.07.007.

Fryirs, K.A., G.J. Brierley, N.J. Preston, and J. Spencer. 2007b. Catchment-scale (dis)connectivity in sediment flux in the upper Hunter catchment, New South Wales, Australia. *Geomorphology* 84, no. 3–4: 297–316. doi:10.1016/j.geomorph.2006.01.044.

Geilhausen, M., D. Morche, J.-C. Otto, and L. Schrott. 2013. Sediment discharge from the proglacial zone of a retreating Alpine glacier. *Zeitschrift Für Geomorphologie, Supplementary Issues* 57, no. 2: 29–53. doi:10.1127/0372-8854/2012/S-00122.

Geilhausen, M., J.-C. Otto, and L. Schrott. 2012. Spatial distribution of sediment storage types in two glacier landsystems (Pasterze & Obersulzbachkees, Hohe Tauern, Austria). *Journal of Maps* 8, no. 3: 242–59. doi:10.1080/17445647.2012.708540.

Haas, F., T. Heckmann, L. Hilger, and M. Becht. 2012. Quantification and modelling of debris flows in the proglacial area of the Gepatschferner, Austria, using ground-based LiDAR. *Presented at the IAHS-AISH Publication*: 293–302. IAHS Publication 356.

Heckmann, T., M. Cavalli, O. Cerdan, S. Foerster, M. Javaux, E. Lode, A. Smetanová, D. Vericat, and F. Brardinoni. 2018. Indices of sediment connectivity: Opportunities, challenges and limitations. *Earth-Science Reviews* 187: 77–108. doi:10.1016/j.earscirev.2018.08.004.

Heckmann, T., D. Morche, and M. Becht. 2019. Introduction. In *Geomorphology of Proglacial Systems*, T. Heckmann and D. Morche, eds. Cham: Springer International Publishing, 1–19.

Heckmann, T., and W. Schwanghart. 2013. Geomorphic coupling and sediment connectivity in an alpine catchment — Exploring sediment cascades using graph theory. *Geomorphology* 182: 89–103. doi:10.1016/j.geomorph.2012.10.033.

Heckmann, T., W. Schwanghart, and J.D. Phillips. 2015. Graph theory—Recent developments of its application in geomorphology. *Geomorphology* 243: 130–46. doi:10.1016/j.geomorph.2014.12.024.

Hiatt, M., E.A. Addink, and M.G. Kleinhans. 2022. Connectivity and directionality in estuarine channel networks. *Earth Surface Processes and Landforms* 47, no. 3: 807–24. doi:10.1002/esp.5286.

Hilger, L. 2017. Quantification and regionalization of geomorphic processes using spatial models and high-resolution topographic data: A sediment budget of the Upper Kauner Valley, Ötztal Alps. Dissertation, Katholische Universität Eichstätt-Ingolstadt: Eichstätt

Hilger, L., J.-M. Dusik, T. Heckmann, F. Haas, P. Glira, N. Pfeifer, L. Vehling, J. Rohn, D. Morche, H. Baewert, M. Stocker-Waldhuber, et al. 2019. A Sediment Budget of the Upper Kaunertal. In *Geomorphology of Proglacial Systems*, T. Heckmann and D. Morche, eds. Cham: Springer International Publishing, 289–312.

Hilger, L., and A.A. Beylich. 2019. Sediment Budgets in High-Mountain Areas: Review and Challenges. In *Geomorphology of Proglacial Systems*, T. Heckmann and D. Morche, eds. Cham: Springer International Publishing, 251–69.

Himmelstoss, T., F. Haas, M. Becht, and T. Heckmann. 2024. Catchment-scale network analysis of functional sediment connectivity during an extreme rainfall event in the Grastal catchment, Austrian Central Alps. *Geomorphology* 465: 109419. doi:10.1016/j.geomorph.2024.109419.

Himmelstoss, T., J. Rom, F. Haas, M. Becht, and T. Heckmann. 2025. Testing the predictive capability of the Index of Connectivity for debris-flow coupling under varying forcing conditions: Insights from two consecutive events in the Horlachtal catchment, Austria. *Earth Surface Processes and Landforms* 50, no. 13: e70173. doi:10.1002/esp.70173.

Hooke, J., and J. Souza. 2021. Challenges of mapping, modelling and quantifying sediment connectivity. *Earth-Science Reviews* 223: 103847. doi:10.1016/j.earscirev.2021.103847.

Kirkbride, M.P., and P. Deline. 2018. Spatial heterogeneity in the paraglacial response to post-Little Ice Age deglaciation of four headwater cirques in the Western Alps. *Land Degradation & Development* 29, no. 9: 3127–40. doi:10.1002/ldr.2975.

Klaar, M.J., C. Kidd, E. Malone, R. Bartlett, G. Pinay, F. S. Chapin, and A. Milner. 2015. Vegetation succession in deglaciated landscapes: Implications for sediment and landscape stability. *Earth Surface Processes and Landforms* 40, no. 8: 1088–100. doi:10.1002/esp.3691.

Knight, J., and S. Harrison. 2014. Mountain glacial and paraglacial environments under global climate change: Lessons from the past, future directions and policy implications. *Geografiska Annaler: Series A, Physical Geography* 96, no. 3: 245–64. doi:10.1111/geoa.12051.

Kuhn, M., E. Schlosser, and N. Span. 1997. Eastern Alpine glacier activity and climatic records since 1860. *Annals of Glaciology* 24: 164–8. doi:10.3189/S0260305500012118.

Lane, S.N., M. Bakker, C. Gabbud, N. Micheletti, and J.-N. Saugy. 2017. Sediment export, transient landscape response and catchment-scale connectivity following rapid climate warming and Alpine glacier recession. *Geomorphology* 277: 210–27. doi:10.1016/j.geomorph.2016.02.015.

Lane, S.N., and P.W. Nienow. 2019. Decadal-Scale Climate Forcing of Alpine Glacial Hydrological Systems. *Water Resources Research* 55, no. 3: 2478–92. doi:10.1029/2018WR024206.

Lehotský, M., M. Rusnák, A. Kidová, and J. Dudžák. 2018. Multitemporal assessment of coarse sediment connectivity along a braided-wandering river. *Land Degradation & Development* 29, no. 4: 1249–61. doi:10.1002/ldr.2870.

Lisenby, P.E., J. Croke, and K.A. Fryirs. 2018. Geomorphic effectiveness: A linear concept in a non-linear world. *Earth Surface Processes and Landforms* 43, no. 1: 4–20. doi:10.1002/esp.4096.

Mancini, D., M. Dietze, T. Müller, M. Jenkin, F. Miesen, M. Roncoroni, A.P. Nicholas, and S.N. Lane. 2023. Filtering of the Signal of Sediment Export From a Glacier by Its Proglacial Forefield. *Geophysical Research Letters* 50, no. 21: e2023GL106082. doi:10.1029/2023GL106082.

Mancini, D., and S.N. Lane. 2020. Changes in sediment connectivity following glacial debuttressing in an Alpine valley system. *Geomorphology* 352: 106987. doi:10.1016/j.geomorph.2019.106987.

Mancini, D., A.P. Nicholas, M. Roncoroni, T. Müller, M. Jenkin, F. Miesen, M. Dietze, F. Calvo, and S.N. Lane. 2025. Simulation of proglacial forefield morphodynamics and their implications for the filtering of subglacial sediment export following glacier retreat. *Earth Surface Processes and Landforms* 50, no. 10: e70143. doi:10.1002/esp.70143.

Mao, L., F. Comiti, R. Carrillo, and D. Penna. 2019. Sediment Transport in Proglacial Rivers. In *Geomorphology of Proglacial Systems*, T. Heckmann and D. Morche, eds. Cham: Springer International Publishing, 199–217.

Martin, S., et al. 2009. Erläuterungen zur geologischen karte von Italien im Maßstab 1: 50.000, Blatt 025 Rabbi. Land Technology & Services, Treviso.

Marty, M., L. Piermattei, L.T. Waser, and C. Ginzler. 2025. Countrywide digital surface models and vegetation height models from historical aerial images. *Earth System Science Data* 17, no. 11: 5811–32. doi:10.5194/essd-17-5811-2025.

Messenzehl, K., T. Hoffmann, and R. Dikau. 2014. Sediment connectivity in the high-alpine valley of Val Müschauns, Swiss National Park — Linking geomorphic field mapping with geomorphometric modelling. *Geomorphology* 221: 215–29. doi:10.1016/j.geomorph.2014.05.033.

Micheletti, N., S.N. Lane, and J.H. Chandler. 2015. Application of archival aerial photogrammetry to quantify climate forcing of alpine landscapes. *The Photogrammetric Record* 30, no. 150: 143–65. doi:10.1111/phor.12099.

Mikolka-Flöry, S., C. Ressl, and N. Pfeifer. 2025. Uncertainty of object points monoplotted from terrestrial images. *PFG – Journal of Photogrammetry, Remote Sensing and Geoinformation Science* 93, no. 6: 645–61. doi:10.1007/s41064-025-00359-6.

Morche, D., H. Baewert, A. Schuchardt, M. Faust, M. Weber, and T. Khan. 2019. Fluvial sediment transport in the proglacial Fagge River, Kaunertal, Austria. In *Geomorphology of Proglacial Systems*, T. Heckmann and D. Morche, eds. Cham: Springer International Publishing, 219–29.

Nuth, C., and A. Kääb. 2011. Co-registration and bias corrections of satellite elevation data sets for quantifying glacier thickness change. *The Cryosphere* 5, no. 1: 271–90. doi:10.5194/tc-5-271-2011.

Orwin, J.F., S.F. Lamoureux, J. Warburton, and A. Beylich. 2010. A framework for characterizing fluvial sediment fluxes from source to sink in cold environments.

Geografiska Annaler: Series A, Physical Geography 92, no. 2: 155–76. doi:10.1111/j.1468-0459.2010.00387.x.

Otto, J., K. Helfricht, G. Prasicek, D. Binder, and M. Keuschnig. 2022. Testing the performance of ice thickness models to estimate the formation of potential future glacial lakes in Austria. *Earth Surface Processes and Landforms* 47, no. 3: 723–41. doi:10.1002/esp.5266.

Phillips, J.D., W. Schwanghart, and T. Heckmann. 2015. Graph theory in the geosciences. *Earth-Science Reviews* 143: 147–60. doi:10.1016/j.earscirev.2015.02.002.

Piermattei, L., T. Heckmann, S. Betz-Nutz, M. Altmann, J. Rom, F. Fleischer, M. Stark, et al. 2023. Evolution of an Alpine proglacial river during 7 decades of deglaciation. *Earth Surface Dynamics* 11, no. 3: 383–403. doi:10.5194/esurf-11-383-2023.

Poeppl, R.E., and A.J. Parsons. 2018. The geomorphic cell: A basis for studying connectivity. *Earth Surface Processes and Landforms* 43, no. 5: 1155–9. doi:10.1002/esp.4300.

Rom, J., S. Betz-Nutz, X. Fan, T. Heckmann, F. Haas, and M. Becht. in review. Morphodynamics in proglacial streams in response to decades of glacier melt. *Arctic, Antarctic, and Alpine Research.*

Rom, J., F. Haas, T. Heckmann, M. Altmann, F. Fleischer, C. Ressl, S. Betz-Nutz, and M. Becht. 2023a. Spatio-temporal analysis of slope-type debris flow activity in Horlachtal, Austria, based on orthophotos and lidar data since 1947. *Natural Hazards and Earth System Sciences* 23, no. 2: 601–22. doi:10.5194/nhess-23-601-2023.

Rom, J., F. Haas, T. Heckmann, F. Dremel, F. Fleischer, M. Altmann, M. Stark, and M. Becht. 2023b. Establishing a record of extreme debris flow events in a high Alpine catchment since the end of the Little Ice Age using lichenometric dating. *Geografiska Annaler: Series A, Physical Geography* 105, no. 1: 47–63. doi:10.1080/04353676.2023.2187531.

Savi, S., A. Buter, T. Heckmann, J. Theule, L. Mao, and F. Comiti. 2023. Multi-temporal analysis of morphological changes in an Alpine proglacial area and their effect on sediment transfer. *Catena* 220: 106701. doi:10.1016/j.catena.2022.106701.

Savi, S., R. Dinale, and F. Comiti. 2021. The Sulden/Solda glacier (Eastern Italian Alps): Fluctuations, dynamics, and topographic control over the last 200 years. *Geografia Fisica E Dinamica Quaternaria* 44: 13–28. doi:10.4461/GFDQ.2021.44.2.

Savi, S., F. Pitscheider, M. Engel, V. Coviello, M.R. Strecker, and F. Comiti. 2024. Sediment export from an Alpine proglacial area under a changing climate: Budgets, rates, and geomorphological processes. *Geomorphology* 462: 109343. doi:10.1016/j.geomorph.2024.109343.

Schmitt, R.J.P., S. Bizzi, and A. Castelletti. 2016. Tracking multiple sediment cascades at the river network scale identifies controls and emerging patterns of sediment connectivity. *Water Resources Research* 52, no. 5: 3941–65. doi:10.1002/2015WR018097.

Schöber, J., and B. Hofer 2018. The sediment budget of the glacial streams in the catchment area of the Gepatsch Reservoir in the Ötztal Alps in the period 1965–2015. Proceedings of ICOLD 2018, Vienna, Austria.

Schwanghart, W., and N.J. Kuhn. 2010. TopoToolbox: A set of Matlab functions for topographic analysis. *Environmental Modelling & Software* 25, no. 6: 770–81. doi:10.1016/j.envsoft.2009.12.002.

Shean, D.E., O. Alexandrov, Z.M. Moratto, B.E. Smith, I. R. Joughin, C. Porter, and P. Morin. 2016. An automated, open-source pipeline for mass production of digital elevation models (DEMs) from very-high-resolution commercial stereo satellite imagery. *ISPRS Journal of Photogrammetry and Remote Sensing* 116: 101–17. doi:10.1016/j.isprsjprs.2016.03.012.

Shi, C., Y. Liang, W. Qin, L. Ding, W. Cao, M. Zhang, and Q. Zhang. 2025. Review of sediment connectivity: Conceptual connotations, characterization indicators, and their relationships with soil erosion and sediment yield. *Earth-Science Reviews* 264: 105091. doi:10.1016/j.earscirev.2025.105091.

Shugar, D.H., J.J. Clague, J.L. Best, C. Schoof, M.J. Willis, L. Copland, and G.H. Roe. 2017. River piracy and drainage basin reorganization led by climate-driven glacier retreat. *Nature Geoscience* 10, no. 5: 370–5. doi:10.1038/ngeo2932.

Staines, K.E.H., J.L. Carrivick, F.S. Tweed, A.J. Evans, A. J. Russell, T. Jóhannesson, and M. Roberts. 2015. A multi-dimensional analysis of pro-glacial landscape change at Sólheimajökull, southern Iceland. *Earth Surface Processes and Landforms* 40, no. 6: 809–22. doi:10.1002/esp.3662.

Stark, M., J. Rom, F. Haas, L. Piermattei, F. Fleischer, M. Altmann, and M. Becht. 2022. Long-term assessment of terrain changes and calculation of erosion rates in an alpine catchment based on SfM-MVS processing of historical aerial images. How camera information and processing strategy affect quantitative analysis. *Journal of Geomorphology*: 101793. doi:10.1127/jgeomorphology/2022/0755.

Steger, S., V. Scorpio, F. Comiti, and M. Cavalli. 2022. Data-driven modelling of joint debris flow release susceptibility and connectivity. *Earth Surface Processes and Landforms* 47, no. 11: 2740–64. doi:10.1002/esp.5421.

Tangi, M., S. Bizzi, K. Fryirs, and A. Castelletti. 2022. A dynamic, network scale sediment (dis)connectivity model to reconstruct historical sediment transfer and river reach sediment budgets. *Water Resources Research* 58, no. 2. doi: 10.1029/2021WR030784.

Tsyplenkov, A., H.G. Smith, H. Betts, and A.J. Neverman. 2025. Data-driven analysis of shallow landslide-to-stream connectivity. *Global and Earth Surface Processes Change* 2: 100002. doi:10.1016/j.gespch.2025.100002.

Turley, M., and M.A. Hassan. 2023. Spatial patterns of disconnectivity explain catchment-scale sediment dynamics and transfer efficiencies. *Journal of Geophysical Research: Earth Surface* 128, no. 6: e2023JF007111. doi:10.1029/2023JF007111.

Turnbull, L., J. Wainwright, and R.E. Brazier. 2008. A conceptual framework for understanding semi-arid land degradation: Ecohydrological interactions across multiple-space and time scales. *Ecohydrology* 1, no. 1: 23–34. doi:10.1002/eco.4.

Veh, G., W. Schwanghart, O. Korup, and J.L. Carrivick. 2026. Evolving resource potential of glacial lakes with ongoing deglaciation. *Nature Water* 4, no. 3: 381–95. doi:10.1038/s44221-025-00578-6.

Vehling, L. 2016. Gravitative massenbewegungen an alpinen felshängen-quantitative bedeutung in der sedimentkaskade proglazialer geosysteme, PhD, Friedrich-Alexander-Universität Erlangen-Nürnberg (FAU)

Vehling, L., H. Baewert, P. Glira, M. Moser, J. Rohn, and D. Morche. 2017. Quantification of sediment transport by rockfall and rockslide processes on a proglacial rock slope (Kaunertal, Austria). *Geomorphology* 287: 46–57. doi:10.1016/j.geomorph.2016.10.032.

Wainwright, J., L. Turnbull, T.G. Ibrahim, I. Lexartza-Artza, S. F. Thornton, and R.E. Brazier. 2011. Linking environmental régimes, space and time: Interpretations of structural and functional connectivity. *Geomorphology* 126, no. 3–4: 387–404. doi:10.1016/j.geomorph.2010.07.027.

Wohl, E., G. Brierley, D. Cadol, T.J. Coulthard, T. Covino, K. A. Fryirs, G. Grant, et al. 2019. Connectivity as an emergent property of geomorphic systems: Geomorphic connectivity. *Earth Surface Processes and Landforms* 44, no. 1: 4–26. doi:10.1002/esp.4434.

Zemp, M., H. Frey, I. Gärtner-roer, S.U. Nussbaumer, M. Hoelzle, F. Paul, W. Haeberli, et al. 2015. Historically unprecedented global glacier decline in the early 21st century. *Journal of Glaciology* 61, no. 228: 745–62. doi:10.3189/2015JoG15J017.

Zhang, T., D. Li, A.E. East, D.E. Walling, S. Lane, I. Overeem, A.A. Beylich, M. Koppes, and X. Lu. 2022. Warming-driven erosion and sediment transport in cold regions. *Nature Reviews Earth & Environment* 3, no. 12: 832–51. doi:10.1038/s43017-022-00362-0.

Zhang, T., W. Wang, and B. An. 2024. Heterogeneous changes in global glacial lakes under coupled climate warming and glacier thinning. *Communications Earth & Environment* 5, no. 1: 374. doi:10.1038/s43247-024-01544-y.

Zheng, G., S.K. Allen, A. Bao, J.A. Ballesteros-Cánovas, M. Huss, G. Zhang, J. Li, et al. 2021. Increasing risk of glacial lake outburst floods from future Third Pole deglaciation. *Nature Climate Change* 11, no. 5: 411–7. doi:10.1038/s41558-021-01028-3.